JOURNAL OF
PHYSICS
AND
CHEMISTRY OF SOLIDS

Subject Index and Chemical Index
Volume 50, 1989

PERGAMON PRESS

OXFORD · NEW YORK
FRANKFURT · SEOUL · SYDNEY · TOKYO

JOURNAL OF PHYSICS AND CHEMISTRY OF SOLIDS

(FOUNDER EDITOR: HARVEY BROOKS)

Editors

A. C. DAMASK, G. J. DIENES and DAVID E. COX,
Editorial Office: *Brookhaven National Laboratory, Upton, NY* 11973, *U.S.A.*

Regional Editors

A. S. BOROVIK-ROMANOV, *Institute of Physical Problems, Academy of Sciences of the U.S.S.R.,* 11734 *Moscow B-334, U.S.S.R.*

JACQUES FRIEDEL, F.R.S., *Laboratoire de Physique des Solides, Bâtiment* 510, *Université de Paris-Sud,* 91405 *Orsay, France*

JOHANN PEISL, *Sektion Physik der Ludwig-Maximilians-Universität München, Geschwister-Scholl-Platz* 1, *D-8000 München* 22, *Germany*

J. M. THOMAS, *Director, Royal Institution, Davy Faraday Laboratory,* 21 *Albemarle Street, London W1X 4BS, U.K.*

GUAN WEIYAN, *University of Science and Technology of China (USTC) at Hefei, China*

Y. YAMADA, *Institute for Solid State Physics, The University of Tokyo, Roppongi, Minato-ku, Tokyo* 106, *Japan*

Editorial Advisory Board

Australasia
L. T. CHADDERTON, Canberra, A.C.T.

Canada
P. W. M. JACOBS, Ontario

China
QINGQUAN GOU, Chengdu, Sichuan

France
E. F. BERTAUT, Grenoble
J. BOK, Paris
B. DREYFUS, Grenoble
A. GUINIER, Orsay
P. HAGENMULLER, Bordeaux
LOUIS NÉEL, Grenoble

Germany
W. HEYWANG, Munich
H. WENZL, Jülich

Italy
F. G. FUMI, Genoa

Japan
K. DATE, Osaka
K. KAWASAKI, Fukuoka

The Netherlands
H. B. G. CASIMIR, Eindhoven

Spain
N. CABRERA, Madrid

Sweden
PER-OLOV LOWDIN, Uppsala

Switzerland
G. BUSCH, Zürich

United Kingdom
C. R. A. CATLOW, London
F. C. FRANK, Bristol
C. L. HONEYBOURNE, Bristol
C. J. HUMPHREYS, Cambridge
A. B. PIPPARD, Cambridge
F. C. TOMPKINS, London

U.S.A.
LEO BREWER, Berkeley, Calif.
E. BURSTEIN, Philadelphia, Penn.
H. K. HENISCH, University Park, Penn.
F. HERMAN, San Jose, Calif.
C. HERRING, Stanford, Calif.
H. B. HUNTINGTON, Troy, N.Y.
C. KITTEL, Berkeley, Calif.
W. KOHN, Santa Barbara, Calif.
J. A. KRUMHANSL, Ithaca, N.Y.
D. PINES, Urbana, Ill.
H. REISS, Los Angeles, Calif.
R. SMOLUCHOWSKI, Austin, Texas
J. TAUC, Providence, R.I.
D. TURNBULL, Cambridge, Mass.
E. P. WIGNER, Princeton, N.J.

U.S.S.R.
G. S. ZHDANOV, Moscow

Publishing, Subscription and Advertising Offices: Pergamon Press plc, Headington Hill Hall, Oxford OX3 0BW, England; and Pergamon Press Inc., Maxwell House, Fairview Park, Elmsford, New York 10523, U.S.A.

Published monthly. Annual institutional subscription rate (1991) DM 1900.00; two-year institutional rate (1991/92) DM 3610.00. Personal subscription rates for those whose library subscribes at the regular rate (1991) please contact your nearest Pergamon office. Subscription rates for Japan include despatch by air and prices are available on application. Prices are subject to change without notice.
Back issues of all previously published volumes, in both hard copy and on microform, are available direct from Pergamon Press offices.

Copyright © 1991 Pergamon Press plc

It is a condition of publication that manuscripts submitted to this journal have not been published and will not be simultaneously submitted or published elsewhere. By submitting a manuscript, the authors agree that the copyright for their article is transferred to the Publisher if and when the article is accepted for publication. However, assignment of copyright is not required from authors who work for organizations which do not permit such assignment. The copyright covers the exclusive rights to reproduce and distribute the article, including reprints, photographic reproductions, microform or any other reproductions of similar nature and translations. No part of this publication may be reproduced, stored in a retrieval system or transmitted in any form or by any means, electronic, electrostatic, magnetic tape, mechanical photocopying, recording or otherwise, without permission in writing from the copyright holder.

PHOTOCOPYING INFORMATION FOR USERS IN THE U.S.A.

The Item-Fee Code for this publication indicates that authorization to photocopy items for internal or personal use is granted by the copyright holder for libraries and other users registered with the Copyright Clearance Center (CCC) Transactional Reporting Service provided the stated fee for copying beyond that permitted by Section 107 or 108 of the United States Copyright law is paid. The appropriate remittance of $3.00 per copy per article is paid directly to the Copyright Clearance Center Inc., 27 Congress Street, Salem, MA 01970.

PERMISSION FOR OTHER USE

The copyright owner's consent does not extend to copying for general distribution, for promotion, for creating new works, or for resale. Specific written permission must be obtained from the Publisher for such copying.

The Item-Fee Code for this publication is: 0022-3697/91 $3.00 + 0.00

♾™ The paper used in this publication meets the minimum requirements of American National Standard for Information Sciences—Permanence of Paper for Printed Library Materials, ANSI Z39.48-1984.

Whilst every effort is made by the publishers and editorial board to see that no inaccurate or misleading data, opinion or statement appear in this journal, they wish to make it clear that the data and opinions appearing in the articles and advertisements herein are the sole responsibility of the contributor or advertiser concerned. Accordingly, the publishers, the editorial board and editors and their respective employees, officers and agents accept no responsibility or liability whatsoever for the consequences of any such inaccurate or misleading data, opinion or statement.

SUBJECT INDEX

Absorption spectra

S. W. Lee, S. K. Ju and J. G. Kang — 69 — Spectroscopic studies of Hg^{2+} color centers in KI single crystal

A. G. Page, S. V. Godbole and M. D. Sastry — 571 — Electronic spectra and co-operative optical transitions in $CaWO_4:Tb^{3+}$ single crystal

S. K. Arora, Thomas Mathew and N. M. Batra — 665 — Optical characterization of $CuWO_4$ single crystals

M. Faucher, D. Garcia, E. Antic-Fidancev and M. Lemaitre-Blaise — 1227 — The spectrum of Nd^{3+} in rare earth orthoaluminates. The trigonal to orthorhombic transition study of the $^2H_{11/2}$ level

Activation energy

Kyung Moon Choi, Keu Hong Kim and Jae Shi Choi — 283 — The chemical and physical properties of electrochemically prepared polyaniline tetrafluoroborates (PATFB)

M. A. K. L. Dissanayake, O. A. Ileperuma and P. A. G. D. Dharmasena — 359 — A.C. conductivity of $MnWO_4$

Don Kim, Kyung Moon Choi, Keu Hong Kim and Jae Shi Choi — 821 — Electrical conductivity of the solid solutions $X Tm_2O_3 + (1 - X)ThO_2$; $0.01 \leqslant X \leqslant 0.15$

Activation enthalpy

M. A. Kashem, J. P. Shukla and S. Walker — 139 — Alkoxycarbonyl group relaxation of some aliphatic esters in glassy media

Alkali halides

A. K. Koh — 39 — Systematic variation of the Szigeti charge in the alkali halides with NaCl structure

W. Kucharczyk — 233 — Ionic sizes in crystals as related to refractive index data

Z. Burshtein — 333 — Comment on "space charge limited current (SCLC) in alkali halide crystals during electrolytic coloration"

W. Kucharczyk — 709 — Photoelastic effect and density derivative of the refractive index in alkali halides

A. Batana and A. D. Castillo — 981 — Pressure dependence of the dielectric properties of alkali halide crystals within the framework of the exchange-charge model

Alkaline-earth compounds

R. C. Baetzold — 915 — Atomistic computation of molecular species in alkaline-earth fluorohalide crystals

Alloys

J. du Plessis and G. N. van Wyk — 237 — A model for surface segregation in multicomponent alloys—Part III: the kinetics of surface segregation in a binary alloy

J. du Plessis and G. N. van Wyk — 247 — A model for surface segregation in multicomponent alloys—Part IV: the kinetics of desegregation in a binary alloy

J. du Plessis and G. N. van Wyk — 251 — A model for surface segregation in multicomponent alloys—Part V: the kinetics of surface segregation in multicomponent alloys

M. J. Ponnambalam — 273 — Effects of a cubically symmetric electron density on the electron field gradient in cubic metal alloys

S. Kawano and N. Achiwa — 353 — Magnetic phase diagram of hcp phases in binary systems between Ho and light rare-earths: La, Ce, Pr

E. D. Belokolos and A. Yu. Gaevsky 1199 The axial Ising model for martensitic transformations and pseudo-elasticity

S. H. Lim, G. E. Murch and W. A. Oates 1251 Thermodynamic properties of ternary alloys from Monte Carlo simulations

Aluminum oxide

D. F. Mariani and M. Jiménez de Castro 125 Thermoluminescent processes in Al_2O_3 X-irradiated at 80 K

L. Badrour, E. G. Moya, J. Bernardini and F. Moya 551 Fast diffusion of silver in single and polycrystals of α-alumina

Aluminophosphates

L. Uytterhoeven, W. J. Mortier and P. Geerlings 479 Charge distribution and effective electro-negativity of aluminophosphate frameworks: influence of the structure type

Aluminum nitride

Kozo Ishizaki and Koji Watari 1009 Oxygen behavior of normal and HIP sintered AlN

Ammonium hydrogen oxalate hemihydrate

Mari Fukai, Takasuke Matsuo and Hiroshi Suga 743 Calorimetric study of phase transitions in ammonium hydrogen oxalate hemihydrate and its deuterated compound

Amorphous materials

F. Picard-Lagnel, B. Poumellec and R. Cortes 1211 Study of amorphous thin films of $(Ti, Nb)O_2$ solid solutions by X-ray absorption at the Ti K edge

Melih Öğmen and Walter W. Duley 1221 Excimer laser deposition of thin amorphous carbon films

Anodic oxidation

S. K. Sharma, B. C. Chakravarty, S. N. Singh, B. K. Das, D. C. Parashar, J. Rai and Prabhat K. Gupta 679 Kinetics of growth of thin anodic oxides of silicon at constant voltages

Antiferromagnets

T. H. Kwon 1083 Dynamical spin correlations in the Oguchi antiferromagnet

Arsenic trisulfide

P. M. Parashak, K. D. Bostic, D. R. Hicks, S. M. Jenkins, John J. Fontanella, Mary C. Wintersgill and C. G. Andeen 867 Effect of pressure on the dielectric constant of arsenic trisulfide glass

Atomic diffusion

Rex B. McLellan 869 Diffusion of the heavy interstitials in metals

Atomic displacements

J. L. Baudour, M. M. Granger, L. Toupet, R. Granger and R. Triboulet 309 Composition dependence of thermal vibrations in $Hg_{1-x}Zn_xTe$ solid solutions determined by X-ray diffraction

Atomic structure

A. Marbeuf, D. Ballutaud, R. Triboulet, H. Dexpert, P. Lagarde and Y. Marfaing 975 EXAFS and XPS studies of $Hg_{1-x}Zn_xTe$: determination of local atomic structure and valence band maximum

Atomistic modelling

A. N. Cormack, C. R. A. Catlow and A. S. Nowick 177 Theoretical studies of off-centre Sc^{3+} impurities in CeO_2

Band structure

L. Komorowski, J. Lipiński and K. Pesz 337 Possible charge-transfer modified band structure of organic conductors

Stephen R. Cain, Luis J. Matienzo and Francis Emmi 87 Modeling of chemical interactions at Cr/Cu interfaces

Bismuth

S. W. Lee, S. K. Ju and J. G. Kang 69 Spectroscopic studies of Hg^{2+} color centers in KI single crystal

H. T. Chu and Yimin Ji 1121 Electron transport phenomena in two-dimensional thin films of pure bismuth

Bismuth telluride

H. Kaibe, Y. Tanaka, M. Sakata and I. Nishida 945 Anisotropic galvanomagnetic and thermoelectric properties of *n*-type Bi_2Te_3 single crystal with the composition of a useful thermoelectric cooling material

Bond lengths

V. Kumar and G. M. Prasad 899 Electronic properties of ionic rocksalt crystals

Borate glass

J. W. M. Verwey, G. F. Imbusch and G. Blasse 813 Laser excited spectroscopy of Gd^{3+} ions in crystalline and glass borate hosts with comparable composition

Boundary layer

J. Ravez, A. Simon, J. P. Bonnet, C. Denage et J. L. Miane 1041 Propriétés diélectriques en hautes fréquences de céramiques à couches d'arrêt de type $SrTiO_3$

Brillouin scattering

C. Ecolivet, A. Miniewicz and M. Sanquer 651 Elastic constants determination in piezoelectric CT complex of carbazole-1,3,5-trinitrobenzene by Brillouin scattering technique

Bulk modulus

J. Freund and R. Ingalls 263 Inverted isothermal equations of state and determination of B_0, B_0' and B_0''

S. K. Saxena and J. Zhang 723 Assessed high-temperature thermochemical data on some solids

Cadmium maleate dihydrate

R. S. Bansal, V. P. Seth and Prem Chand 839 EPR study of vanadyl ion in cadmium maleate dihydrate single crystals

Cadmium stannate

Clay M. Cardile 221 ^{119}Sn Mössbauer spectroscopy of cadmium stannates

Cadmium tungstate

Z. Burshtein and J. Ivri 1271 Davydov splitting and two-photon excitation of cadmium tungstate ($CsWO_4$) single crystal phosphorescence

Calorimetry

Hitoshi Kawaji, Tooru Atake and Yasutoshi Saito 215 Heat capacities, magnetic phase transition at 42.02 K and order–disorder phase transition at 673 K of $AgCrS_2$

C. Picard and P. Gerdanian 383 Thermodynamics of $Co_{1-\delta}O$

E. H. P. Cordfunke, R. J. M. Konings, E. F. Westrum, Jr and R. Shaviv 429 The thermophysical and thermochemical properties of RuO_2 from 0 to 1000 K

N. B. Chanh, J. R. Housty, A. Meresse, L. Ricard and M. Rey-Lafon 829 Polymorphism in the bidimensional compound $(n\text{-}C_{16}H_{33}NH_3)_2CdCl_4$

Carbides

A. L. Ivanovsky, V. I. Anisimov and V. A. Gubanov 883 The influence of structural defects on the electronic properties of interstitial alloys—IV. The electronic structure of 3*d*-, 4*d*-metallic impurities in ScC, TiC, VC and ZrC

Carbon

Melih Öğmen and Walter W. Duley 1221 Excimer laser deposition of thin amorphous carbon films

Carbon–nitrogen austenite

C. Ko and Rex B. McLellan 619 Thermodynamics of C–N austenites

Catalysts

G. T. Kokotailo and C. A. Fyfe 441 Perspective: Zeolites; unique materials for research and industry

Cation distribution

Jozef J. Van Dun, Kristine Dhaeze, Wilfried J. Mortier and David E. W. Vaughan — 469 — The influence of isomorphous substitution on the cation distribution in faujasite-type zeolites; the structures of dehydrated Na-LZ210 and hydrated KGaY

K. Petrov, K. Krezhov and P. Konstantinov — 577 — Neutron diffraction study of the cationic distribution in $Cu_xCo_{3-x}O_4 (0 \leqslant x \leqslant 1.0)$ spinels prepared by thermal decomposition of layered hydroxide nitrate precursors

Cation doping

Edmond C. Akubuiro and Xenophon E. Verykios — 17 — Effects of altervalent cation doping on electrical conductivity of platinized titania

Cation vacancies

J. Grammatikakis, C. A. Londos, V. Katsika and N. Bogris — 845 — Migration enthalpy of the cation vacancies in $LiF:Be^{2+}$

Cesium nitroprusside

M. M. Vergara, E. L. Varetti, G. Rigotti and A. Navaza — 951 — The crystalline and molecular structure and the vibrational spectra of anhydrous cesium nitroprusside

Chain structures

D. Welz, P. Deppe, W. Schaefer, H. Sabrowsky and M. Rosenberg — 297 — Magnetism of iron–sulfur tetrahedral frameworks in compounds with thallium. I. Chain structures

Chalcogenide compounds

W. Kucharczyk — 233 — Ionic sizes in crystals as related to refractive index data

Gabriel Jasiolek, Zbigniew Golacki and Marek Godlewski — 277 — X-ray characterization of precipitates in HgTe:Eu and ZnS:Eu crystals

P. M. Parashak, K. D. Bostic, D. R. Hicks, S. M. Jenkins, John J. Fontanella, Mary C. Wintersgill and C. G. Andeen — 867 — Effect of pressure on the dielectric constant of arsenic trisulfide glass

Charge transfer

L. Komorowski, J. Lipiński and K. Pesz — 337 — Possible charge-transfer modified band structure of organic conductors

G. Blasse — 99 — The europium(III)–fluorine charge-transfer transition

A. C. Pavão and J. P. B. da Silva — 669 — Electronic structure and charge-transfer transitions in $(NiF_6)^{4-}$

Jamila Ghamri, Hervé Baussart, Michel Le Bras and Jean-Marie Leroy — 1237 — Spectroscopic study of $Bi_xEu_{1-x}VO_4$ and $Bi_yGd_{1-y}VO_4$ mixed oxides

Charge transport

Jean-Louis Carpentier, André Lebrun and Francis Perdu — 145 — Point defects and charge transport in pure and chromium-doped rutile at 1273 K

Chemical shifts

R. A. Nissan and T. A. Vanderah — 347 — ^{31}P Solid state NMR studies of ZrP, Mg_3P_2, MgP_4 and $CdPS_3$

A. F. Privalov, H.-M. Vieth and I. V. Murin — 395 — Ionic motion in the LaF_3 superionic conductor studied by ^{19}F NMR with homonuclear decoupling

Chemical vapor deposition

Miki Niwa and Yuichi Murakami — 487 — CVD zeolites with controlled pore-opening size

Chemisorption

H. Lechert and W. D. Basler — 497 — Molecular motion in zeolite sorbends, studied by various NMR methods

Chromium

P. J. Alonso, R. Alcalá, J. Casas-Gonzalez, R. Cases and V. M. Orera — 1185 — Spectroscopy of chromium(III) in yttrium-stabilized ZrO_2

Chromium compounds

Jean-Louis Carpentier, André Lebrun and Francis Perdu — 145 — Point defects and charge transport in pure and chromium-doped rutile at 1273 K

Chromium/copper interfaces

Stephen R. Cain, Luis J. Matienzo and Francis Emmi 87 Modeling of chemical interactions at Cr/Cu interfaces

Chrysoberyl

Z. Burshtein, D. O. Henderson, S. Morgan and E. Silberman 1095 Vibrational spectra of chrysoberyl ($BeAl_2O_4$)

Co-operative transitions

A. G. Page, S. V. Godbole and M. D. Sastry 571 Electronic spectra and co-operative optical transitions in $CaWO_4$: Tb^{3+} single crystal

Cobalt monoxide

C. Picard and P. Gerdanian 383 Thermodynamics of $Co_{1-\delta}O$

Cobalt phosphides

Manfred Reehuis and Wolfgang Jeitschko 563 Magnetic properties of lanthanoid iron and cobalt phosphides with $Zr_2Fe_{12}P_7$ type structure

Coherency strain

A. F. Jankowski 641 The strain wave approach to modulus enhancement and stability of metallic multilayers

Color centers

J. Minge and J. A. Weil 997 ^{57}Fe hyperfine structure of $[FeO_4/Li]^0$ center in α-quartz

Computer simulation

A. N. Cormack, C. R. A. Catlow and A. S. Nowick 177 Theoretical studies of off-centre Sc^{3+} impurities in CeO_2

R. C. Baetzold, C. R. A. Catlow, J. Corish, F. M. Healy, P. W. M. Jacobs, M. Leslie and Y. T. Tan 791 The effects of three-body interactions on crystal properties and defect energies in silver halides

S. H. Lim, G. E. Murch and W. A. Oates 1251 Thermodynamic properties of ternary alloys from Monte Carlo simulations

Conducting polymers

A. Morin, M. Bénière and F. Bénière 611 Diffusion of $FeCl_4$ in polyacetylene

Copper

Sangeetha Sampath, R. R. Tripathi and M. P. Tare 921 Structural and electrical properties of $CoCuSnO_4$ prepared by two different methods

Donald Greenspan 1245 Supercomputer simulation of cracks and fractures by quasimolecular dynamics

Copper oxide

Michael M. Rigney, Charles P. Poole, Jr and H. A. Farach 9 Average copper charge and valence states of superconducting copper-oxides

Coumarine

Tadashi Endo, Nobuyuki Nakada, Tsugio Sata and Massahiko Shimada 133 The fluorescence properties of coumarine dye intercalated in a swelling clay

Covalent bond resonance

A. C. Pavão and J. P. B. da Silva 669 Electronic structure and charge-transfer transitions in $(NiF_6)^{4-}$

Cracks

Donald Greenspan 1245 Supercomputer simulation of cracks and fractures by quasimolecular dynamics

Cristobalite

G. L. Hua, T. R. Welberry and R. L. Withers 207 Lattice dynamics of α- and β-cristobalite, SiO_2

Crystal defects

K. R. Udayakumar and A. N. Cormack 55 Non-stoichiometry in alkaline earth excess alkaline earth titanates

Seok Ho Yun, Keu Hong Kim and Jae Shi Choi 291 Defect structure and electrical conductivity of pure and doped lutetium sesquioxides

A. Halperin 407 The low temperature phosphorescence and thermoluminescence of X-rayed Ge-doped quartz

A. Jovanović, M. Wöhlecke, S. Kapphan, A. Maillard and G. Godefroy 623 Infrared spectroscopy of hydrogen centers in undoped and iron-doped $BaTiO_3$ crystals

Sheikh A. Akbar and Hiroshi Sato 729 Demixing: a source of material deterioration

R. C. Baetzold, C. R. A. Catlow, J. Corish, F. M. Healy, P. W. M. Jacobs, M. Leslie and Y. T. Tan 791 The effects of three-body interactions on crystal properties and defect energies in silver halides

R. C. Baetzold 915 Atomistic computation of molecular species in alkaline-earth fluorohalide crystals

P. P. Lottici, G. Antonioli and C. Razzetti 967 Ordered-vacancy compound semiconductors: an EXAFS study of the structure of α-$CdIn_2Se_4$

H. Y. Ueng and H. L. Hwang 1297 The defect structure of $CuInS_2$. Part I: Intrinsic defects

K. R. Udayakumar and A. N. Cormack 55 Non-stoichiometry in alkaline earth excess alkaline earth titanates

Crystal field analysis

M. Faucher, D. Garcia, E. Antic-Fidancev and M. Lemaitre-Blaise 1227 The spectrum of Nd^{3+} in rare earth orthoaluminates. The trigonal to orthorhombic transition study of the $^2H_{11/2}$ level

N. Nagasundaram and A. H. Francis 163 FTIR electronic spectra of $Fe_2P_2S_6$ and $Co_2P_2S_6$: trigonal field splitting and lithium intercalation effects

Crystal structure

Jozef J. Van Dun, Kristine Dhaeze, Wilfried J. Mortier and David E. W. Vaughan 469 The influence of isomorphous substitution on the cation distribution in faujasite-type zeolites; the structures of dehydrated Na-LZ210 and hydrated KGaY

M. M. Vergara, E. L. Varetti, G. Rigotti and A. Navaza 951 The crystalline and molecular structure and the vibrational spectra of anhydrous cesium nitroprusside

J. Zaleski, T. Glowiak, R. Jakbus and L. Sobczyk 1265 Crystal structure and phase transitions of $[(C_2H_5)_4N]_6Bi_8Cl_{30}$

Cuprous iodide

Ruben A. Montani and Julio C. Bazán 1207 On the potential range of applicability of Wagner's polarization method

Curie temperatures

Manfred Reehuis and Wolfgang Jeitschko 563 Magnetic properties of lanthanoid iron and cobalt phosphides with $Zr_2Fe_{12}P_7$ type structure

Davydov splitting

Z. Burshtein, D. O. Henderson, S. Morgan and E. Silberman 1095 Vibrational spectra of chrysoberyl ($BeAl_2O_4$)

Z. Burshtein and J. Ivri 1271 Davydov splitting and two-photon excitation of cadmium tungstate ($CsWO_4$) single crystal phosphorescence

Defects

A. N. Cormack, C. R. A. Catlow and A. S. Nowick 177 Theoretical studies of off-centre Sc^{3+} impurities in CeO_2

A. Jovanović, M. Wöhlecke, S. Kapphan, A. Maillard and G. Godefroy 623 Infrared spectroscopy of hydrogen centers in undoped and iron-doped $BaTiO_3$ crystals

A. L. Ivanovsky, V. I. Anisimov and V. A. Gubanov 883 The influence of structural defects on the electronic properties of interstitial alloys—IV. The electronic structure of 3*d*-, 4*d*-metallic impurities in ScC, TiC, VC and ZrC

Yoshimi Watanabe, A. Sato and T. Mura 957 Growth of a nitrogen defect cluster in a bcc lattice examined by a lattice theory

T. Miki, M. R. Hantehzadeh and L. E. Halliburton 1003 A new trapped-hole center in irradiated $LiNbO_3$

H. Y. Ueng and H. L. Hwang 1297 The defect structure of $CuInS_2$. Part I: Intrinsic defects

Demixing

Sheikh A. Akbar and Hiroshi Sato 729 Demixing: a source of material deterioration

Density functional theory

Shinichi Ichikawa 931 Superconductivity and optimum electronegativity

Density of states

L. Komorowski, J. Lipiński and K. Pesz 337 Possible charge-transfer modified band structure of organic conductors

C. L. Roy 111 Relativistic electronic states of disordered systems

S. R. Dhariwal and P. T. Landsberg 363 A theoretical study of field-enhanced emission (Poole–Frenkel effect)

Desegregation

D. du Plessis and G. N. van Wyk 237 A model for surface segregation in multicomponent alloys—Part III: the kinetics of surface segregation in a binary alloy

D. du Plessis and G. N. van Wyk 247 A model for surface segregation in multicomponent alloys—Part IV: the kinetics of desegregation in a binary alloy

D. du Plessis and G. N. van Wyk 251 A model for surface segregation in multicomponent alloys—Part V: the kinetics of surface segregation in multicomponent alloys

Dielectric properties

J. Grammatikakis, C. A. Londos, V. Katsika and N. Bogris 845 Migration enthalpy of the cation vacancies in $LiF:Be^{2+}$

P. M. Parashak, K. D. Bostic, D. R. Hicks, S. M. Jenkins, John J. Fontanella, Mary C. Wintersgill and C. G. Andeen 867 Effect of pressure on the dielectric constant of arsenic trisulfide glass

V. Kumar and G. M. Prasad 899 Electronic properties of ionic rocksalt crystals

A. Batana and A. D. Castillo 981 Pressure dependence of the dielectric properties of alkali halide crystals within the framework of the exchange-charge model

J. Ravez, A. Simon, J. P. Bonnet, C. Denage et J. L. Miane 1041 Propriétés diélectriques en hautes fréquences de céramiques à couches d'arrêt de type $SrTiO_3$

B. K. Chaudhuri, K. Chaudhuri and K. K. Som 1149 Concentration and frequency dependences of a.c. conductivity and dielectric constant of iron–bismuth oxide glasses—II

Dielectric relaxation

M. A. Kashem, J.P. Shukla and S. Walker 139 Alkoxycarbonyl group relaxation of some aliphatic esters in glassy media

John Gilchrist 857 Low temperature dielectric relaxations in ammonium hexachlorostannate and some other antifluorites

Rachel Howe and R. W. Whitworth 963 The electrical conductivity of KOH-doped ice from 70 to 250 K

Syuji Kawada 1177 Acceleration of dielectric relaxation by KOH-doping and phase transition in ice Ih

Diffraction

J. M. Thomas and D. E. W. Vaughan 449 Methodologies to establish the structure and composition of new zeolitic molecular sieves

Diffuse reflectance spectroscopy (DRS)

Robert A. Schoonheydt 523 Combined ESR–DRS spectroscopies of transition metal ions and metal ion clusters in zeolites

Diffusion

Rex B. McLellan 49 The thermodynamics of hybrid binary interstitial–substitutional solid solutions

J. du Plessis and G. N. van Wyk 237 A model for surface segregation in multicomponent alloys—Part III: the kinetics of surface segregation in a binary alloy

D. du Plessis and G. N. van Wyk 247 A model for surface segregation in multicomponent alloys—Part IV: the kinetics of desegregation in a binary alloy

D. du Plessis and G. N. van Wyk 251 A model for surface segregation in multicomponent alloys—Part V: the kinetics of surface segregation in multicomponent alloys

L. Badrour, E. G. Moya, J. Bernardini and F. Moya 551 Fast diffusion of silver in single and polycrystals of α-alumina

A. Morin, M. Bénière and F. Bénière 611 Diffusion of $FeCl_4^-$ in polyacetylene

Sheikh A. Akbar and Hiroshi Sato 729 Demixing: a source of material deterioration

L. Bonpunt, A. Dautant, A. Loumaïd and F. Fauré 777 2-Naphthole lattice diffusion at infinite dilution in naphthalene single crystals—I: diffusion tensor—influence of the purity of the naphthalene

Rex B. McLellan 869 Diffusion of the heavy interstitials in metals

Yoshimi Watanabe, A. Sato and T. Mura 957 Growth of a nitrogen defect cluster in a bcc lattice examined by a lattice theory

Rex B. McLellan and Franz R. Brotzen 1045 The effect of oxygen interstitial doping on "fast" diffusion in α-titanium

Disordered systems

C. L. Roy 111 Relativistic electronic states of disordered systems

Dispersion relations

C. L. Hua, T. R. Welberry and R. L. Withers 207 Lattice dynamics of α- and β-cristobalite, SiO_2

Dynamical motion

P. S. R. Prasad and H. D. Bist 1033 Vibrational spectroscopic study of the structural phase transitions in perovskite layer compounds $(CH_3NH_3)_2CdCl_4$

Elastic constants

C. Ecolivet, A. Miniewicz and M. Sanquer 651 Elastic constants determination in piezoelectric CT complex of carbazole-1,3,5-trinitrobenzene by Brillouin scattering technique

Richard Barber, Micah Downing, James B. Shaw and L. S. Cain 1077 The second-order elastic constants of AgBr–AgCl mixed crystals from 77 to 300 K

V. Hadjicontis, K. Eftaxias and C. Varotsos 1193 Connection between the Birch equation of state and the Schottky formation volume in NaCl

Elastic moduli

A. F. Jankowski 641 The strain wave approach to modulus enhancement and stability of metallic multilayers

Elastic strain

Keishi Negita and Hiroshi Takao 325 Condensations of phonons at the tetragonal to monoclinic phase transition in ZrO_2

Electric field gradient

M. J. Ponnambalam 273 Effects of a cubically symmetric electron density on the electric field gradient in cubic metal alloys

Electric modulus

Partho Sarkar and **Patrick S. Nicholson** 197 Electric field relaxation studies in the CeO_2–Y_2O_3 system

Electrical conduction

Jean-Louis Carpentier, André Lebrun and **Francis Perdu** 145 Point defects and charge transport in pure and chromium-doped rutile at 1273 K

Electrical conductivity

Jong Sik Park, Kyung Moon Choi, Keu Hong Kim and **Jae Shi Choi** 909 Electrical conductivity of the solid solutions $X ThO_2 + (1-X) Ho_2O_3$; $0.02 \leqslant X \leqslant 0.10$

L. Komorowski, J. Lipiński and **K. Pesz** 337 Possible charge-transfer modified band structure of organic conductors

R. J. Thorn and **C. E. Thorn** 153 Semiconductive and semimetallic components in superconducting oxides: effect of oxidation

Edmond C. Akubuiro and **Xenophon E. Verykios** 17 Effects of altervalent cation doping on electrical conductivity of platinized titania

Jean-Louis Carpentier, André Lebrun and **Francis Perdu** 145 Point defects and charge transport in pure and chromium-doped rutile at 1273 K

Clay M. Cardile 221 ^{119}Sn Mössbauer spectroscopy of cadmium stannates

Seok Ho Yun, Keu Hong Kim and **Jae Shi Choi** 291 Defect structure and electrical conductivity of pure and doped lutetium sesquioxides

S. Fujita, A. Garcia, D. O'Leyar, S. Watanabe and **T. Burnett** 27 On the conductance of a lattice-like network

M. A. K. L. Dissanayake, O. A. Ileperuma and **P. A. G. D. Dharmasena** 359 A.C. conductivity of $MnWO_4$

H. R. Ries, W. L. Harries, S. A. T. Long and **E. R. Long, Jr** 735 Mechanism of electrical conductivity in an irradiated polyimide

Don Kim, Kyung Moon Choi, Keu Hong Kim and **Jae Shi Choi** 821 Electrical conductivity of the solid solutions $X Tm_2O_3 + (1 - X) ThO_2$; $0.01 \leqslant X \leqslant 0.15$

Yoo Young Kim, Keu Hong Kim and **Jae Shi Choi** 903 Infrared spectra and electrical conductivity of the α-Fe_2O_3–B_2O_3 system

Sangeetha Sampath, R. R. Tripathi and **M. P. Tare** 921 Structural and electrical properties of $CoCuSnO_4$ prepared by two different methods

Rachel Howe and **R. W. Whitworth** 963 The electrical conductivity of KOH-doped ice from 70 to 250 K

Keu Hong Kim, Do Young Kim, Kyung Moon Choi, Jae Shi Choi and **Robert G. Sauer** 1027 Electrical conductivity of the solid solutions $X Gd_2O_3 + (1 - X) ThO_2$; $0.01 \leqslant X \leqslant 0.12$

Biswanath Mallik and **Ashis Bhattacharjee** 1113 Adsorption-induced unusual changes in the electrical conductivity of ferrocene

H. T. Chu and **Yimin Ji** 1121 Electron transport phenomena in two-dimensional thin films of pure bismuth

B. K. Chaudhuri, K. Chaudhuri and **K. K. Som** 1137 Concentration dependences of d.c. conductivity of the iron–bismuth oxide glasses—I

B. K. Chaudhuri, K. Chaudhuri and **K. K. Som** 1149 Concentration and frequency dependences of a.c. conductivity and dielectric constant of iron–bismuth oxide glasses—II

J. C. Bernede, G. Safoula, R. Messoussi, A. Bonnet and **A. Conan** 1169 Electrical properties of iodine-doped selenium films

Ruben A. Montani and **Julio C. Bazán** 1207 On the potential range of applicability of Wagner's polarization method

Keu Hong Kim, Do Young Kim, Kyung Moon Choi, Jae Shi Choi and **Robert G. Sauer** 1027 Electrical conductivity of the solid solutions $X Gd_2O_3 + (1 - X) ThO_2$; $0.01 \leqslant X \leqslant 0.12$

Don Kim, Kyung Moon Choi, Keu Hong Kim and Jae Shi Choi — 821 — Electrical conductivity of the solid solutions $X\mathrm{Tm_2O_3} + (1 - X)\mathrm{ThO_2}$; $0.01 \leqslant X \leqslant 0.15$

Electrical properties

Kyung Moon Choi, Keu Hong Kim and Jae Shi Choi — 283 — The chemical and physical properties of electrochemically prepared polyaniline tetrafluoroborates (PATFB)

R. Benloucif, N. Nguyen, J. M. Greneche and B. Raveau — 435 — $\mathrm{La_{2-2x}Sr_{2x}Ni_{1-x}Fe_xO_{4-(x/2)+\delta}}$: magnetic and electron transport properties

J. Misiewicz — 1013 — Optical and electrical investigations of imperfection levels in $\mathrm{Zn_3P_2}$

Electrical transport

H. T. Chu and Yimin Ji — 1121 — Electron transport phenomena in two-dimensional thin films of pure bismuth

Electroconduction

R. M. Mostovoy, V. Ya. Sukharev, V. I. Berendyayev, B. V. Kotov and I. A. Myasnikov — 541 — Structural chemical characteristics and electroconduction mechanism of polymeric ion-radical TCNQ salts based on aliphatic ionenes

Electrode kinetics

Laura E. Fasano and Julio C. Bazán — 259 — A theoretical model for silver ion transfer through the solid–solid Ag/AgI interface

Electron density

M. J. Ponnambalam — 273 — Effects of a cubically symmetric electron density on the electric field gradient in cubic metal alloys

Electron transport

Jong Ho Jun, Sung Han Lee, Keu Hong Kim and Jae Shi Choi — 785 — Electron transport in polyvinylchloride–magnetite composites

Electronegativity

A. K. Koh — 39 — Systematic variation of the Szigeti charge in the alkali halides with NaCl structure

L. Uytterhoeven, W. J. Mortier and P. Geerlings — 479 — Charge distribution and effective electronegativity of aluminophosphate frameworks: influence of the structure type

Shinichi Ichikawa — 931 — Superconductivity and optimum electronegativity

Chikara Sugiura, Michihide Kitamura and Shinji Muramatsu — 1069 — Chlorine $K\beta$ X-ray emission spectra from selected transition-metal complex compounds

Electron adsorption

N. Nagasundaram and A. H. Francis — 163 — FTIR electronic spectra of $\mathrm{Fe_2P_2S_6}$ and $\mathrm{Co_2P_2S_6}$: trigonal field splitting and lithium intercalation effects

Electronic properties

V. Kumar and G. M. Prasad — 899 — Electronic properties of ionic rocksalt crystals

A. Charlier, M. F. Charlier and D. Fristot — 987 — Binary graphite intercalation compounds

Geneviève Volpilhac et Francis Achard — 1163 — Un moyen de calculer les propriétés électroniques des molécules en interaction avec un solide

Electronic spectra

A. G. Page, S. V. Godbole and M. D. Sastry — 571 — Electronic spectra and co-operative optical transitions in $\mathrm{CaWO_4}$: $\mathrm{Tb^{3+}}$ single crystal

J. Swanepoel — 935 — The distorted *trans*-octahedral molecular geometry of iron(II) difluoride tetrahydrate

Electronic states

C. L. Roy — 111 — Relativistic electronic states of disordered systems

Electronic structure

E. J. D. Garba and **R. L. Jacobs** 101 The electronic structures of Fe_3C and Ni_3B

A. C. Pavão and **J. P. B. da Silva** 669 Electronic structure and charge-transfer transitions in $(NiF_6)^{4-}$

Eric Sandré, Raymond Brec and **Jean Rouxel** 801 Electronic structure of MX_2-type layered compounds

A. L. Ivanovsky, V. I. Anisimov and **V. A. Gubanov** 883 The influence of structural defects on the electronic properties of interstitial alloys—IV. The electronic structure of 3*d*-, 4*d*-metallic impurities in ScC, TiC, VC and ZrC

Emission spectra

S. W. Lee, S. K. Ju and **J. G. Kang** 69 Spectroscopic studies of Hg^{2+} color centers in KI single crystal

Energy bands

E. J. D. Garba and **R. L. Jacobs** 101 The electronic structures of Fe_3C and Ni_3B

Energy gap

A. M. Elkorashy 893 Temperature dependence of the optical energy gap in tin monoselenide single crystals

Energy transfer

B. C. Joshi and **U. C. Pandey** 599 Interaction between Tb^{3+} and Er^{3+} ions in phosphate glass

Jamila Ghamri, Hervé Baussart, Michel Le Bras and **Jean-Marie Leroy** 1237 Spectroscopic study of $Bi_xEu_{1-x}VO_4$ and $Bi_yGd_{1-y}VO_4$ mixed oxides

J. P. M. van Vliet and **G. Blasse** 1277 Luminescence and energy transfer in europium tellurite anti-glass phases

Entropy

E. H. P. Cordfunke, R. J. M. Konings, E. F. Westrum, Jr and **R. Shaviv** 429 The thermophysical and thermochemical properties of RuO_2 from 0 to 1000 K

EPR

F. Callens, P. Matthys and **E. Boesman** 377 Paramagnetic resonance spectrum of CO_2^- trapped in KCl

R. S. Bansal, V. P. Seth and **Prem Chand** 839 EPR study of vanadyl ion in cadmium maleate dihydrate single crystals

J. Minge and **J. A. Weil** 997 ^{57}Fe hyperfine structure of $[FeO_4/Li]^0$ center in α-quartz

Sushil K. Misra, Kingsley Mbaebie and **S. Subramanian** 1157 Doublet separations of forbidden-hyperfine transitions in the EPR of transition-metal complexes

P. J. Alonso, R. Alcalá, J. Casas-Gonzalez, R. Cases and **V. M. Orera** 1185 Spectroscopy of chromium(III) in yttrium-stabilized ZrO_2

Equation of state

Jens W. Otto, Richard F. Porter and **Arthur L. Ruoff** 171 Equation of state of solid ammonia (NH_3) to 56 GPa

J. Freund and **R. Ingalls** 263 Inverted isothermal equations of state and determination of B_0, B_0' and B_0''

V. Hadjicontis, K. Eftaxias and **C. Varotsos** 1193 Connection between the Birch equation of state and the Schottky formation volume in NaCl

ESR

Robert A. Schoonheydt 523 Combined ESR–DRS spectroscopies of transition metal ions and metal ion clusters in zeolites

T. Miki, M. R. Hantehzadeh and **L. E. Halliburton** 1003 A new trapped-hole center in irradiated $LiNbO_3$

Europium

G. Blasse 99 The europium(III)–fluorine charge-transfer transition

EXAFS

A. Marbeuf, D. Ballutaud, R. Triboulet, H. Dexpert, P. Lagarde and Y. Marfaing 975 EXAFS and XPS studies of $Hg_{1-x}Zn_xTe$: determination of local atomic structure and valence band maximum

P. P. Lottici, G. Antonioli and C. Razzetti 967 Ordered-vacancy compound semiconductors: an EXAFS study of the structure of α-$CdIn_2Se_4$

Exchange-charge model

A. Batana and A. D. Castillo 981 Pressure dependence of the dielectric properties of alkali halide crystals within the framework of the exchange-charge model

Excitons

Yuan-Ping Feng, Zhilan Huang and Harold N. Spector 117 Ionization cross section of excitons due to scattering by free carriers in semiconducting quantum well structures

R. Ruppin 877 Optical absorption by excitons in microcrystals

Fergusonite

Jamila Ghamri, Hervé Baussart, Michel Le Bras and Jean-Marie Leroy 1237 Spectroscopic study of $Bi_xEu_{1-x}VO_4$ and $Bi_yGd_{1-y}VO_4$ mixed oxides

Fermi energy

Edmond C. Akubuiro and Xenophon E. Verykios 17 Effects of altervalent cation doping on electrical conductivity of platinized titania

Fermi level

E. J. D. Garba and R. L. Jacobs 101 The electronic structures of Fe_3C and Ni_3B

Fermi liquid

F. Steglich 225 Heavy fermions

Ferrocene

Biswanath Mallik and Ashis Bhattacharjee 1113 Adsorption-induced unusual changes in the electrical conductivity of ferrocene

Ferroelectricity

R. Poprawski and A. Kolarz 693 Thermally stimulated light emission from the linear pyroelectric and ferroelectric surfaces

Zuo-Guang Ye, Régnault Von Der Mühll et Jean Ravez 809 New oxyfluorides and highly densified ceramics related to $LiNbO_3$

Field-enhanced emission

S. R. Dhariwal and P. T. Landsberg 363 A theroetical study of field-enhanced emission (Poole–Frenkel effect)

Fluorescence

Tadashi Endo, Nobuyuki Nadada, Tsugio Sato and Masahiko Shimada 133 The fluorescence properties of coumarine dye intercalated in a swelling clay

A. G. Page, S. V. Godbole and M. D. Sastry 571 Electronic spectra and co-operative optical transitions in $CaWO_4:Tb^{3+}$ single crystal

B. C. Joshi and U. C. Pandey 599 Interaction between Tb^{3+} and Er^{3+} ions in phosphate glass

J. W. M. Verwey, G. F. Imbusch and G. Blasse 813 Laser excited spectroscopy of Gd^{3+} ions in crystalline and glass borate hosts with comparable composition

Z. Burshtein and J. Ivri 1271 Davydov splitting and two-photon excitation of cadmium tungstate ($CsWO_4$) single crystal phosphorescence

Fluorides

G. Blasse 99 The europium(III)–fluorine charge-transfer transition

A. F. Privalov, H.-M. Vieth and **I. V. Murin** 395 Ionic motion in the LaF_3 superionic conductor studied by ^{19}F NMR with homonuclear decoupling

Fluorite oxides

Partho Sarkar and **Patrick S. Nicholson** 197 Electric field relaxation studies in the CeO_2–Y_2O_3 system

Forbidden-hyperfine transitions

Sushil K. Misra, Kingsley Mbaebie and **S. Subramanian** 1157 Doublet separations of forbidden-hyperfine transitions in the EPR of transition-metal complexes

Fracture

Donald Greenspan 1245 Supercomputer simulation of cracks and fractures by quasimolecular dynamics

Free carriers

Yuan-Ping Feng, Zhilan Huang and **Harold N. Spector** 117 Ionization cross section of excitons due to scattering by free carriers in semiconducting quantum well structures

Free energy

S. K. Saxena and **J. Zhang** 723 Assessed high-temperature thermochemical data on some solids

Kozo Ishizaki and **Koji Watari** 1009 Oxygen behavior of normal and HIP sintered AlN

Galvanomagnetic properties

H. Kaibe, Y. Tanaka, M. Sakata and **I. Nishida** 945 Anisotropic galvanomagnetic and thermoelectric properties of *n*-type Bi_2Te_3 single crystal with the composition of a useful thermoelectric cooling material

Gamma–alpha transformation

François Mathieu and **Abel Rousset** 61 Study of the $\gamma \rightarrow \alpha$ transformation occurring in finely divided γ-Fe_2O_3 in the presence of water and under high pressure (viz. 5.5 GPa)—mechanism of oxyhydroxides formation

Gibbs–Duhem equation

D. J. Young, F. Viani and **F. Gesmundo** 415 Effect of the deviation from stoichiometry on the activity of pure oxides and of oxide solid solutions

Glass transition

N. Okamoto, M. Oguni and **H. Suga** 1285 Calorimetric study of thiophene–benzene solutions(I)

Grain boundaries

L. Badrour, E. G. Moya, J. Bernardini and **F. Moya** 551 Fast diffusion of silver in single and polycrystals of α-alumina

J. Ravez, A. Simon, J. P. Bonnet, C. Denage et **J. L. Miane** 1041 Propriétés diélectriques en hautes fréquences de céramiques à couches d'arrêt de type $SrTiO_3$

Graphite

A. Charlier, M. F. Charlier and **D. Frisot** 987 Binary graphite intercalation compounds

Geneviève Volpilhac et **Francis Achard** 1163 Un moyen de calculer les propriétés électroniques des molécules en interaction avec un solide

Green matrix

Geneviève Volpilhac et **Francis Achard** 1163 Un moyen de calculer les propriétés électroniques des molécules en interaction avec un solide

Growth kinetics

S. K. Sharma, B. C. Chakravarty, S. N. Singh, B. K. Das, D. C. Parashar, J. Rai and **Prabhat K. Gupta** 679 Kinetics of growth of thin anodic oxides of silicon at constant voltages

Hall effect

H. T. Chu and **Yimin Ji** 1121 Electron transport phenomena in two-dimensional thin films of pure bismuth

Heat capacity

Hitoshi Kawaji, Tooru Atake and Yasutoshi Saito — 215 — Heat capacities, magnetic phase transition at 42.02 K and order–disorder phase transition at 673 K of $AgCrS_2$

K. Chhor, L. Abello and C. Pommier — 423 — Low temperature calorimetric and Raman spectrometric studies on lithium ammonium sulphate, $LiNH_4SO_4$

E. H. P. Cordfunke, R. J. M. Konings, E. F. Westrum, Jr and R. Shaviv — 429 — The thermophysical and thermochemical properties of RuO_2 from 0 to 1000 K

Masanori Yoshikawa, Michio Sorai and Hiroshi Suga — 713 — Heat capacity of a five-coordinated iron(III) complex with spin $S = 3/2$, bromobis (N, N-dimethyldithiocarbamato) iron(III), between 0.4 and 300 K: new finding of a magnetic phase transition

S. K. Saxena and J. Zhang — 723 — Assessed high-temperature thermochemical data on some solids

Mari Fukai, Takasuke Matsuo and Hiroshi Suga — 743 — Calorimetric study of phase transitions in ammonium hydrogen oxalate hemihydrate and its deuterated compound

J. L. Hock and R. B. McQuistan — 1051 — Constant coverage configurational heat capacities for two-dimensional square-cell lattices

N. Okamoto, M. Oguni and H. Suga — 1285 — Calorimetric study of thiophene–benzene solutions(I)

Heavy fermions

F. Steglich — 225 — Heavy fermions

Heisenberg antiferromagnet

T. H. Kwon — 1083 — Dynamical spin correlations in the Oguchi antiferromagnet

Helium

Rex B. McLellan — 49 — The thermodynamics of hybrid binary interstitial–substitutional solid solutions

High pressure studies

François Mathieu and Abel Rousset — 61 — Study of the $\gamma \rightarrow \alpha$ transformation occurring in finely divided γ-Fe_2O_3 in the presence of water and under high pressure (viz. 5.5 GPa)—mechanism of oxyhydroxides formation

J. Freund and R. Ingalls — 263 — Inverted isothermal equations of state and determination of B_0, B_0' and B_0''

R. A. Dalterio and F. J. Owens — 739 — Raman study of high pressure induced phase transition in sodium nitrite

L. S. de Oliveira, M. T. X. Silva and J. A. H. da Jornada — 763 — Temperature and pressure effects on the iron carbides formed by carbon ion implantation

Steven J. Duclos, A. Jayaraman, G. P. Espinosa, A. S. Cooper and R. G. Maines, Sr — 769 — Raman and optical absorption studies of the pressure-induced zircon to scheelite structure transformation in $TbVO_4$ and $DyVO_4$

P. M. Parashak, K. D. Bostic, D. R. Hicks S. M. Jenkins, John J. Fontanella, Mary C. Wintersgill and C. G. Andeen — 867 — Effect of pressure on the dielectric constant of arsenic trisulfide glass

Kozo Ishizaki and Koji Watari — 1009 — Oxygen behavior of normal and HIP sintered AIN

Hopping conduction

Kyung Moon Choi, Keu Hong Kim and Jae Shi Choi — 283 — The chemical and physical properties of electrochemically prepared polyaniline tetrafluoroborates (PATFB)

R. M. Mostovoy, V. Ya. Sukharev, V. I. Berendyayev, B. V. Kotov and I. A. Myasnikov — 541 — Structural chemical characteristics and electroconduction mechanism of polymeric ion-radical TCNQ salts based on aliphatic ionenes

B. K. Chaudhuri, K. Chaudhuri and K. K. Som — 1149 — Concentration and frequency dependences of a.c. conductivity and dielectric constant of iron–bismuth oxide glasses—II

Hybridization

E. J. D. Garbar and **R. L. Jacobs** 101 The electronic structures of Fe_3C and Ni_3B

Hydrogen bonding

P. S. R. Prasad and **H. D. Bist** 1033 Vibrational spectroscopic study of the structural phase transitions in perovskite layer compounds $(CH_3NH_3)_2CdCl_4$

Hydrogen fluorides

P. L. Crouse 369 A conversion electron Mössbauer spectroscopic study of the reactions between hydrogen fluoride and iron oxide surface films in the presence and absence of oxygen and water vapour

Hyperfine interaction

J. Minge and **J. A. Weil** 997 ^{57}Fe hyperfine structure of $[FeO_4/Li]^0$ center in α-quartz

Ice

Rachel Howe and **R. W. Whitworth** 963 The electrical conductivity of KOH-doped ice from 70 to 250 K

Syuji Kawada 1177 Acceleration of dielectric relaxation by KOH-doping and phase transition in ice Ih

Impurities

A. N. Cormack, C. R. A. Catlow and **A. S. Nowick** 177 Theoretical studies of off-center Sc^{3+} impurities in CeO_2

A. Halperin 407 The low temperature phosphorescence and thermoluminescence of X-rayed Ge-doped quartz

L. Bonpunt, A. Dautant, A. Loumaïd and **F. Fauré** 777 2-Naphthole lattice diffusion at infinite dilution in naphthalene single crystals—I. diffusion tensor—influence of the purity of the naphthalene

J. Minge and **J. A. Weil** 997 ^{57}Fe hyperfine structure of $[FeO_4/Li]^0$ center in α-quartz

Impurity levels

J. Misiewicz 1013 Optical and electrical investigations of imperfection levels in Zn_3P_2

Indium oxides

Tery L. Barr and **Ying Li Liu** 657 An X-ray photoelectron spectroscopy study of the valence band structure of indium oxides

Infrared spectroscopy

El-Metwally Nour and **Maha Jabor Al Thani** 183 Preparation and infrared spectra of $(Cu(O)(H_2O)_3)$ and $(Cu_2(O)(Cl)_2(H_2O)_2)$ complexes formed in the reactions of Cu(II) salts with urea

A. Jovanović, M. Wöhlecke, S. Kapphan, A. Maillard and **G. Godefroy** 623 Infrared spectroscopy of hydrogen centers in undoped and iron-doped $BaTiO_3$ crystals

J. W. M. Verwey, G. F. Imbusch and **G. Blasse** 813 Laser excited spectroscopy of Gd^{3+} ions in crystalline and glass borate hosts with comparable composition

Yoo Young Kim, Keu Hong Kim and **Jae Shi Choi** 903 Infrared spectra and electrical conductivity of the α-Fe_2O_3–B_2O_3 system

M. M. Vergara, E. L. Varetti, G. Rigotti and **A. Navaza** 951 The crystalline and molecular structure and the vibrational spectra of anhydrous cesium nitroprusside

P. S. R. Prasad and **H. D. Bist** 1033 Vibrational spectroscopic study of the structural phase transitions in perovskite layer compounds $(CH_3NH_3)_2CdCl_4$

Z. Burshtein, D. O. Henderson, S. Morgan and **E. Silberman** 1095 Vibrational spectra of chrysoberyl ($BeAl_2O_4$)

B. K. Chaudhuri, K. Chaudhuri and **K. K. Som** 1137 Concentration dependences of d.c. conductivity of the iron–bismuth oxide glasses—I

J. Swanepoel 935 The distorted *trans*-octahedral molecular geometry of iron(II) difluoride tetrahydrate

Intercalation compounds

Tadashi Endo, Nobuyuki Nakada, Tgugio Sato and Masahiko Shimada — 133 — The fluorescence properties of coumarine dye intercalated in a swelling clay

N. Nagasundaram and A. H. Francis — 163 — FTIR electronic spectra of $Fe_2P_2S_6$ and $Co_2P_2S_6$: trigonal field splitting and lithium intercalation effects

A. Charlier, M. F. Charlier and D. Fristot — 987 — Binary graphite intercalation compounds

Interfaces

Stephen R. Cain, Luis J. Matienzo and Francis Emmi — 87 — Modeling of chemical interactions at Cr/Cu interfaces

Laura E. Fasano and Julio C. Bazán — 259 — A theoretical model for silver ion transfer through the solid–solid Ag/AgI interface

Interlayer interactions

E. D. Belokolos and A. Yu. Gaevsky — 1199 — The axial Ising model for martensitic transformations and pseudo-elasticity

Intermetallic compounds

F. Steglich — 225 — Heavy fermions

Regina Krachler, Herbert Ipser and Kurt L. Komarek — 1127 — Thermodynamics of intermetallic B2-phases. A generalized model

Interstitial compounds

Rex B. McLellan — 49 — The thermodynamics of hybrid binary interstitial–substitutional solid solutions

A. L. Ivanovsky, V. I. Anisimov and V. A. Gubanov — 883 — The influence of structural defects on the electronic properties of interstitial alloys—IV. The electronic structure of 3*d*-, 4*d*-metallic impurities in ScC, TiC, VC and ZrC

D. Sundararaman, S. Raju and V. S. Raghunathan — 1101 — Theoretical analysis of interstitial ordering and precipitation processes in the Ti–N system

Interstitial defects

Rex B. McLellan and Franz R. Brotzen — 1045 — The effect of oxygen interstitial doping on "fast" diffusion in α-titanium

Rex B. McLellan — 869 — Diffusion of the heavy interstitials in metals

Iodine

J. C. Bernede, G. Safoula, R. Messoussi, A. Bonnet and A. Conan — 1169 — Electrical properties of iodine-doped selenium films

Ion implantation

L. S. de Oliveira, M. T. X. Silva and J. A. H. da Jornada — 763 — Temperature and pressure effects on the iron carbides formed by carbon ion implantation

Ion transfer

Laura E. Fasano and Julio C. Bazán — 259 — A theoretical model for silver ion transfer through the solid–solid Ag/AgI interface

Ionenes

R. M. Mostovoy, V. Ya. Sukharev, V. I. Berendyayev, B. V. Kotov and I. A. Myasnikov — 541 — Structural chemical characteristics and electroconduction mechanism of polymeric ion-radical TCNQ salts based on aliphatic ionenes

Ionic conductivity

Z. Burshtein — 333 — Comment on "space charge limited current (SCLC) in alkali halide crystals during electrolytic coloration"

Partho Sarkar and Patrick S. Nicholson — 197 — Electric field relaxation studies in the CeO_2–Y_2O_3 system

J. Grammatikakis, C. A. Londos, V. Katsika and N. Bogris 845 Migration enthalpy of the cation vacancies in $LiF:Be^{2+}$

V. Hadjicontis, K. Eftaxias and C. Varotsos 1193 Connection between the Birch equation of state and the Schottky formation volume in NaCl

Ionic mobility

A. F. Privalov, H.-M. Vieth and I. V. Murin 395 Ionic motion in the LaF_3 superionic conductor studied by ^{19}F NMR with homonuclear decoupling

Ionic radii

W. Kucharczyk 233 Ionic sizes in crystals as related to refractive index data

Ionicity

A. K. Koh 39 Systematic variation of the Szigeti charge in the alkali halides with NaCl structure

Ionization cross section

Yuan-Ping Feng, Zhilan Huang and Harold N. Spector 117 Ionization cross section of excitons due to scattering by free carriers in semiconducting quantum well structures

Ionization energies

H. Y. Ueng and H. L. Hwang 1297 The defect structure of $CuInS_2$. Part I: Intrinsic defects

Iron

R. Gerardin, H. Aqachmar, I. Nodari, J. F. Brice et O. Evrard 43 Contribution a l'etude du système Lu_2O_3–Mn_2O_3–Fe_2O_3 et caractérisation de deux varietés cristallographiques de $Lu_2Mn_2Fe_2O_9$

Iron compounds

François Mathieu and Abel Rousset 61 Study of the $\gamma \rightarrow \alpha$ transformation occurring in finely divided γ-Fe_2O_3 in the presence of water and under high pressure (vis. 5.5 GPa)—mechanism of oxyhydroxides formation

D. Welz, P. Deppe. W. Schaefer, H. Sabrowsky and M. Rosenberg 297 Magnetism of iron–sulfur tetrahedral frameworks in compounds with thallium. I. Chain structures

P. L. Crouse 369 A conversion electron Mössbauer spectroscopic study of the reactions between hydrogen fluoride and iron oxide surface films in the presence and absence of oxygen and water vapour

Masanori Yoshikawa, Michio Sorai and Hiroshi Suga 713 Heat capacity of a five-coordinated iron(III) complex with spin $S = 3/2$, bromobis (*N*,*N*-dimethyldithiocarbamato) iron(III), between 0.4 and 300 K: new finding of a magnetic phase transition

L. S. de Oliveira, M. T. X. Silva and J. A. H. da Jornada 763 Temperature and pressure effects on the iron carbides formed by carbon ion implantation

J. Swanepoel 935 The distorted *trans*-octahedral molecular geometry of iron(II) difluoride tetrahydrate

Irradiation

H. R. Ries, W. L. Harries, S. A. T. Long and E. R. Long, Jr 735 Mechanism of electrical conductivity in an irradiated polyimide

R. C. Baetzold 915 Atomistic computation of molecular species in alkaline-earth fluorohalide crystals

Ising model

E. D. Belokolos and A. Yu. Gaevsky 1199 The axial Ising model for martensitic transformations and pseudoelasticity

Isomorphous substitution

Jozef J. Van Dun, Kristine Dhaeze, Wilfried J. Mortier and David E. W. Vaughan 469 The influence of isomorphous substitution on the cation distribution in faujasite-type zeolites; the structures of dehydrated Na-LZ210 and hydrated KGaY

Isotopic engineering

Alexander A. Berezin 5 Isotopic engineering

Jahn–Teller effect

S. W. Lee, S. K. Ju and J. G. Kang 69 Spectroscopic studies of Hg^{2+} color centers in KI single crystal

Robert A. Schoonheydt 523 Combined ESR–DRS spectroscopies of transition metal ions and metal ion clusters in zeolites

H. Donker, W. M. A. Smit and G. Blasse 603 On the luminescence of Te^{4+} in A_2ZrCl_6(A = Cs, Rb) and A_2SnCl_6 (A = Cs, Rb, K)

Lanthanoid iron phosphides

Manfred Reehuis and Wolfgang Jeitsckko 563 Magnetic properties of lanthanoid iron and cobalt phosphides with $Zr_2Fe_{12}P_7$ type structure

Laser deposition

Melih Ögmen and Walter W. Duley 1221 Excimer laser deposition of thin amorphous carbon films

Lattice constants

W. Kucharczyk 233 Ionic sizes in crystals as related to refractive index data

Lattice coverage

J. L. Hock and R. B. McQuistan 1051 Constant coverage configurational heat capacities for two-dimensional square-cell lattices

Lattice dilation

Rex B. McLellan and Franz R. Brotzen 1045 The effect of oxygen interstitial doping on "fast" diffusion in α-titanium

Lattice dynamics

G. L. Hua, T. R. Welberry and R. L. Withers 207 Lattice dynamics of α- and β-cristobalite, SiO_2

Keishi Negita and Hiroshi Takao 325 Condensations of phonons at the tetragonal to monoclinic phase transition in ZrO_2

Lattice expansion

Peter Adler, Harmut Spiering and Philipp Gütlich 587 Thermodynamics and kinetics of spin state conversion processes studied by pressure dependent Mössbauer spectroscopy

Lattice gas

S. H. Lim, G. E. Murch and W. A. Oates 1251 Thermodynamic properties of ternary alloys from Monte Carlo simulations

Lattice modes

R. A. Dalterio and F. J. Owens 739 Raman study of high pressure induced phase transition in sodium nitrite

Lattice statistics

J. L. Hock and R. B. McQuistan 1051 Constant coverage configurational heat capacities for two-dimensional square-cell lattices

Lattice theory

Yoshimi Watanabe, A. Sato and T. Mura 957 Growth of a nitrogen defect cluster in a bcc lattice examined by a lattice theory

Lattice-like circuits

S. Fujita, A. Garcia, D. O'Leyar, S. Watanabe and T. Bennett 27 On the conductance of a lattice-like network

Layered compounds

Eric Sandré, Raymond Brec and Jean Rouxel 801 Electronic structure of MX_2-type layered compounds

Ligand field

Robert A. Schoonheydt 523 Combined ESR–DRS spectroscopies of transition metal ions and metal ion clusters in zeolites

Light emission

R. Poprawski and **A. Kolarz** 693 Thermally stimulated light emission from the linear pyroelectric and ferroelectric surfaces

Lithium

Geneviève Volpilhac et **Francis Achard** 1163 Un moyen de calculer les propriétés électroniques des molécules en interaction avec un solide

Lithium ammonium sulphate

Y. A. Badr and **S. B. El-Guiziri** 1261 Effect of γ-radiation on the phase transition temperature of $Li_{0.5}(NH_4)_{0.5}SO_4$

Lithium niobate

T. Miki, M. R. Hantehzadeh and **L. E. Halliburton** 1003 A new trapped-hole center in irradiated $LiNbO_3$

Lithium properties

Eric Sandré, Raymond Brec and **Jean Rouxel** 801 Electronic structure of MX_2-type layered compounds

Low-dimensional properties

Shoichi Nagata, Hiroki Kutsuzawa, Shuji Ebisu, Hidemi Yamamura and **Satoshi Taniguchi** 703 Superconductivity in the quasi-one-dimensional conductor $TaSe_3$

Low-dimensional magnet

Masanori Yoshikawa, Michio Sorai and **Hiroshi Suga** 713 Heat capacity of a five-coordinated iron(III) complex with spin $S = 3/2$, bromobis (N,N-dimethyldithiocarbamato) iron(III), between 0.4 and 300 K: new finding of a magnetic phase transition

Luminescence

R. Stoyanova, S. Angelov and **R. Dafinova** 95 Identification of the center of self-activated luminescence in strontium carbonate by doping with lithium

G. Blasse, J. P. M. van Vliet, J. W. M. Verwey, R. Hoogendam and **M. Wiegel** 583 Luminescence of Pr^{3+} in scandium borate ($ScBO_3$) and the host lattice dependence of the Stokes shift

H. Donker, W. M. A. Smit and **G. Blasse** 603 On the luminescence of Te^{4+} in A_2ZrCl_6(A = Cs,Rb) and A_2SnCl_6 (A = Cs, Rb, K)

W. Ryba-Romanowski, S. Gołąb, J. Hanuza and **M. Berkowski** 685 Relaxation of the $^4F_{3/2}$ level of Nd^{3+} in $BaLa_{1-x}Nd_xGa_3O_7$

J. W. M. Verwey, G. F. Imbusch and **G. Blasse** 813 Laser excited spectroscopy of Gd^{3+} ions in crystalline and glass borate hosts with comparable composition

R. C. Baetzold 915 Atomistic computation of molecular species in alkaline-earth fluorohalide crystals

Lutetium ferrites

R. Gerardin, H. Aqachmar, I. Nodari, J. F. Brice et **O. Evrard** 43 Contribution a l'étude du système Lu_2O_3–Mn_2O_3–Fe_2O_3 et caractérisation de deux varietés cristallographiques de $Lu_2Mn_2Fe_2O_9$

Magnetic ordering

L. Tákacs and **W. M. Reiff** 33 Three-dimensional magnetic ordering of $K_2FeH_5 \cdot H_2O$: Mössbauer spectroscopy investigation in the helium-3 temperature range

F. Steglich 225 Heavy fermions

H. Fjellvåg, A. Kjekshus, R. Zach and **A. Zięba** 187 $Mn_{1-t}(Ti_{0.50}V_{0.50})_tAs$; diluted manganese monoarsenide with zero overall chemical pressure

Hitoshi Kawaji, Tooru Atake and **Yasutoshi Saito** 215 Heat capacities, magnetic phase transition at 42.02 K and order-disorder phase transition at 673 K of $AgCrS_2$

S. Kawano and N. Achiwa 353 Magnetic phase diagram of hcp phases in binary systems between Ho and light rare-earths: La, Ce, Pr

S. Kawano 633 Neutron diffraction study of hcp erbium–lanthanum alloys

Masanori Yoshikawa, Michio Sorai and Hiroshi Suga 713 Heat capacity of a five-coordinated iron(III) complex with spin $S = 3/2$, bromobis (*N,N*-dimethyldithiocarbamato) iron(III), between 0.4 and 300 K: new findings of a magnetic phase transition

Magnetic properties

D. Welz, P. Deppe, W. Schaefer, H. Sabrowsky and M. Rosenberg 297 Magnetism of iron–sulfur tetrahedral frameworks in compounds with thallium. I. Chain structures

R. Benloucif, N. Nguyen, J. M. Greneche and B. Raveau 435 $La_{2-2x}Sr_{2x}Ni_{1-x}Fe_xO_{4-(x/2)+\delta}$: magnetic and electron transport properties

Manfred Reehuis and Wolfgang Jeitschko 563 Magnetic properties of lanthanoid iron and cobalt phosphides with $Zr_2Fe_{12}P_7$ type structure

F. Fernández, R. Sáez-Puche, C. Cascales, C. M. Marcano and I. Rasines 871 X-ray diffraction data and magnetic properties of the oxides $R_3Sb_5O_{12}$ (R = Pr, Nd, Sm, Eu, Gd, Yb)

Magnetic relaxation

Karin Larsson, Jörgen Tegenfeldt and Åke Kvick 107 NMR study of the motion of water molecules in the natural zeolite bikitaite

Magnetite

Jong Ho Jun, Sung Han Lee, Keu Hong Kim and Jae Shi Choi 785 Electron transport in polyvinylchloride–magnetite composites

Manganese compounds

H. Fjellvåg, A. Kjekshus, R. Zach and A. Zięba 187 $Mn_{1-t}(Ti_{0.50}V_{0.50})_tAs$; diluted manganese monoarsenide with zero overall chemical pressure

R. Gerardin, H. Aqachmar, I. Nodari, J. F. Brice et O. Evrard 43 Contribution a l'étude du système Lu_2O_3–Mn_2O_3–Fe_2O_3 et caractérisation de deux varietés cristallographiques de $Lu_2Mn_2Fe_2O_9$

M. A. K. L. Dissanayake, O. A. Ileperuma and P. A. G. D. Dharmasena 359 A.C. conductivity of $MnWO_4$

Martensitic transformations

E. D. Belokolos and A. Yu. Gaevsky 1199 The axial Ising model for martensitic transformations and pseudoelasticity

Mercury–zinc telluride

A. Marbeuf, D. Ballutaud, R. Triboulet, H. Dexpert, P. Lagarde and Y. Marfaing 975 EXAFS and XPS studies of $Hg_{1-x}Zn_xTe$: determination of local atomic structure and valence band maximum

Metallic impurities

A. L. Ivanovsky, V. I. Anisimov and V. A. Gubanov 883 The influence of structural defects on the electronic properties of interstitial alloys—IV. The electronic structure of 3*d*-, 4*d*-metallic impurities in ScC, TiC, VC and ZrC

Microcrystals

R. Ruppin 877 Optical absorption by excitons in microcrystals

Migration enthalpy

J. Grammatikakis, C. A. Londos, V. Katsika and N. Bogris 845 Migration enthalpy of the cation vacancies in $LiF:Be^{2+}$

Mixed crystals

Richard Barber, Micah Downing, James B. Shaw and L. S. Cain 1007 The second-order elastic constants of AgBr–AgCl mixed crystals from 77 to 300 K

Mixed valence

R. Benloucif, N. Nguyen, J. M. Greneche and B. Raveau 435 $La_{2-2x}Sr_{2x}Ni_{1-x}Fe_xO_{4-(x/2)+\delta}$: magnetic and electron transport properties

Mode coupling

P. S. R. Prasad and **H. D. Bist** 1033 Vibrational spectroscopic study of the structural phase transitions in perovskite layer compounds $(CH_3NH_3)_2\ CdCl_4$

Mode softening

Joanne R. Rollo and **Gary R. Burns** 753 Temperature dependences of the Raman spectra of the tetraphosphorus triselenodiiodides (α'-$P_4Se_3I_2$ and β-$P_4Se_3I_2$) and the tetraphosphorus trithiodiiodides (α-$P_4S_3I_2$ and β-$P_4S_3I_2$)

Molecular crystals

L. Bonpunt, A. Dautant, A. Loumaïd and **F. Fauré** 777 2-Naphthole lattice diffusion at infinite dilution in naphthalene single crystals—I: diffusion tensor—influence of the purity of the naphthalene

Molecular geometry

J. Swanepoel 935 The distorted *trans*-octahedral molecular geometry of iron(II) difluoride tetrahydrate

Molecular interactions

Geneviève Volpilhac et **Francis Achard** 1163 Un moyen de calculer les propriétés électroniques des molécules en interaction avec un solide

Molecular motion

H. Lechert and **W. D. Basler** 497 Molecular motion in zeolite sorbends, studied by various NMR methods

Molecular sieves

J. M. Thomas and **D. E. W. Vaughan** 449 Methodologies to establish the structure and composition of new zeolitic molecular sieves

L. Uytterhoeven, W. J. Mortier and **P. Geerlings** 479 Charge distribution and effective electronegativity of aluminophosphate frameworks: influence of the structure type

Molecular structure

M. M. Vergara, E. L. Varetti, G. Rigotti and **A. Navaza** 951 The crystalline and molecular structure and the vibrational spectra of anhydrous cesium nitroprusside

Monte Carlo simulations

S. H. Lim, G. E. Murch and **W. A. Oates** 1251 Thermodynamic properties of ternary alloys from Monte Carlo simulations

Mordenite

Miki Niwa and **Yuichi Murakami** 487 CVD zeolites with controlled pore-opening size

Mössbauer spectroscopy

L. Takács and **W. M. Reiff** 33 Three-dimensional magnetic ordering of $K_2FeF_5 \cdot H_2O$: Mössbauer spectroscopy investigation in the helium-3 temperature range

R. Gerardin, H. Aqachmar, I. Nodari, J. F. Brice et **O. Evrard** 43 Contribution a l'étude de système Lu_2O_3–Mn_2O_3–Fe_2O_3 et caractérisation de deux varietés cristallographiques de $Lu_2Mn_2Fe_2O_9$

Clay M. Cardile 221 ^{119}Sn Mössbauer spectroscopy of cadmium stannates

D. Welz, P. Deppe, W. Schaefer, H. Sabrowsky and **M. Rosenberg** 297 Magnetism of iron–sulfur tetrahedral frameworks in compounds with thallium. I. Chain structures

P. L. Crouse 369 A conversion electron Mössbauer spectroscopic study of the reactions between hydrogen fluoride and iron oxide surface films in the presence and absence of oxygen and water vapour

R. Benloucif, N. Nguyen, J. M. Greneche and **B. Raveau** 435 $La_{2-2x}Sr_{2x}Ni_{1-x}Fe_xO_{4-(x/2)+\delta}$: magnetic and electron transport properties

Peter Adler, Harmut Spiering and **Philipp Gütlich** 587 Thermodynamics and kinetics of spin state conversion processes studied by pressure dependent Mössbauer spectroscopy

L. S. de Oliveira, M. T. X. Silva and J. A. H. da Jornada 763 Temperature and pressure effects on the iron carbides formed by carbon ion implantation

J. Swanepoel 935 The distorted *trans*-octahedral molecular geometry of iron(II) difluoride tetrahydrate

G. Alonzo, L. Garbato, F. Ledda and C. Muntoni 1195 121-antimony Mössbauer spectroscopic study on some antimony–tellurium alloys

Multilayers

A. F. Jankowski 641 The strain wave approach to modulus enhancement and stability of metallic multilayers

Naphthalene

L. Bonpunt, A. Dautant, A. Loumaïd and F. Fauré 777 2-Naphthole lattice diffusion at infinite dilution in naphthalene single crystals—I: diffusion tensor—influence of the purity of the naphthalene

Neodymium compounds

W. Ryba-Romanowski, S. Gołąb, J. Hanuza and M. Berkowski 685 Relaxation of the $^4F_{3/2}$ level of Nd^{3+} in $BaLa_{1-x}Nd_xGa_3O_7$

M. Faucher, D. Garcia, E. Antic-Fidancev and M. Lemaitre-Blaise 1227 The spectrum of Nd^{3+} in rare earth orthoaluminates. The trigonal to orthorhombic transition study of the $^2H_{11/2}$ level

Neutron diffraction

S. Kawano and N. Achiwa 353 Magnetic phase diagram of hcp phases in binary systems between Ho and light rare-earths: La, Ce, Pr

K. Petrov, K. Krezhov and P. Konstantinov 577 Neutron diffraction study of the cationic distribution in $Cu_xCo_{3-x}O_4 (0 \leqslant x \leqslant 1.0)$ spinels prepared by thermal decomposition of layered hydroxide nitrate precursors

S. Kawano 633 Neutron diffraction study of hcp erbium–lanthanum alloys

Neutron scattering

D. Welz, P. Deppe, W. Schaefer, H. Sabrowsky and M. Rosenberg 297 Magnetism of iron–sulfur tetrahedral frameworks in compounds with thallium. I. Chain structures

T. H. Kwon 1083 Dynamical spin correlations in the Oguchi antiferromagnet

Nitrogen

D. Sundararaman, S. Raju and V. S. Raghunathan 1101 Theoretical analysis of interstitial ordering and precipitation processes in the Ti–N system

NMR

Karin Larsson, Jörgen Tegenfeldt and Åke Kvick 107 NMR study of the motion of water molecules in the natural zeolite bikitaite

R. A. Nissan and T. A. Vanderah 347 ^{31}P solid state NMR studies of ZrP, Mg_3P_2, MgP_4 and $CdPS_3$

G. T. Kokotailo and C. A. Fyfe 441 Perspective: Zeolites; unique materials for research and industry

H. Lechert and W. D. Basler 497 Molecular motion in zeolite sorbends, studied by various NMR methods

Non-stoichiometry

K. R. Udayakumar and A. N. Cormack 55 Non-stoichiometry in alkaline earth excess alkaline earth titanates

C. Picard and P. Gerdanian 383 Thermodynamics of $Co_{1-\delta}O$

D. J. Young, F. Viani and F. Gesmundo 415 Effect of the deviation from stoichiometry on the activity of pure oxides and of oxide solid solutions

Optical properties

D.F. Mariani and M. Jiménez de Castro 125 Thermoluminescent processes in Al_2O_3 X-irradiated at 80 K

J. R. Sambles 1 Optical excitation of surface plasmons

N. V. Joshi, J. C. Sanchez and J. M. Martin — 629 Photoconducting properties of InP:Fe

S. K. Arora, Thomas Mathew and N. M. Batra — 665 Optical characterization of $CuWO_4$ single crystals

Steven J. Duclos, A. Jayaraman, G. P. Espinosa, A. S. Cooper and R. G. Maines, Sr — 769 Raman and optical absorption studies of the pressure-induced zircon to scheelite structure transformation in $TbVO_4$ and $DyVO_4$

R. Ruppin — 877 Optical absorption by excitons in microcrystals

A. M. Elkorashy — 893 Temperature dependence of the optical energy gap in tin monoselenide single crystals

H. C. Gupta, Geeta Sood, Arvind Parashar and B. B. Tripathi — 925 Long wavelength optical lattice vibrations in mixed chalcogenide spinels $Zn_{1-x}Cd_xCr_2S_4$ and $CdCr_2(S_{1-x}Se_x)_4$

J. Misiewicz — 1013 Optical and electrical investigations of imperfection levels in Zn_3P_2

Optical sensors

J. R. Sambles — 1 Optical excitation of surface plasmons

Optoelectronics

Alexander A. Berezin — 5 Isotopic engineering

Organic conductors

L. Komorowski, J. Lipiński and K. Pesz — 337 Possible charge-transfer modified band structure of organic conductors

R. M. Mostovoy, V. Ya. Sukharev, V. I. Berendyayev, B. V. Kotov and I. A. Myasnikov — 541 Structural chemical characteristics and electroconduction mechanism of polymeric ion-radical TCNQ salts based on aliphatic ionenes

Oscillators

Rex B. McLellan — 869 Diffusion of the heavy interstitials in metals

Oxidation

R. J. Thorn and C. E. Thorn — 153 Semiconductive and semimetallic components in superconducting oxides: effect of oxidation

Clay M. Cardile — 221 ^{119}Sn Mössbauer spectroscopy of cadmium stannates

H. Verweij and W. H. M. Bruggink — 75 Constant stoichiometry cooling of $YBa_2Cu_3O_x$

Oxide activity

D. J. Young, F. Viani and F. Gesmundo — 415 Effect of the deviation from stoichiometry on the activity of pure oxides and of oxide solid solutions

Oxide compounds

R. J. Thorn and C. E. Thorn — 153 Semiconductive and semimetallic components in superconducting oxides: effect of oxidation

Partho Sarkar and Patrick S. Nicholson — 197 Electric field relaxation studies in the CeO_2–Y_2O_3 system

D. J. Young, F. Viani and F. Gesmundo — 415 Effect of the deviation from stoichiometry on the activity of pure oxides and of oxide solid solutions

K. Petrov, K. Krezhov and P. Konstantinov — 577 Neutron diffraction study of the cationic distribution in $Cu_xCo_{3-x}O_4 (0 \leqslant x \leqslant 1.0)$ spinels prepared by thermal decomposition of layered hydroxide nitrate precursors

Don Kim, Kyung Moon Choi, Keu Hong Kim and Jae Shi Choi — 821 Electrical conductivity of the solid solutions $X Tm_2O_3 + (1 - X)ThO_2$; $0.01 \leqslant X \leqslant 0.15$

Keu Hong Kim, Do Young Kim, Kyung Moon Choi, Jae Shi Choi and Robert G. Sauer — 1027 Electrical conductivity of the solid solutions $X Gd_2O_3 + (1 - X)ThO_2$; $0.01 \leqslant X \leqslant 0.12$

P. J. Alonso, R. Alcalá, J. Casas-Gonzalez, R. Cases and V. M. Orera 1185 Spectroscopy of chromium(III) in yttrium-stabilized ZrO_2

Jong Sik Park, Kyung Moon Choi, Keu Hong Kim and Jae Shi Choi 909 Electrical conductivity of the solid solutions $X ThO_2 + (1 - X)Ho_2O_3$; $0.02 \leqslant X \leqslant 0.10$

Seok Ho Yun, Keu Hong Kim and Jae Shi Choi 291 Defect structure and electrical conductivity of pure and doped lutetium sesquioxides

Oxide glasses

B. K. Chaudhuri, K. Chaudhuri and K. K. Som 1137 Concentration dependences of d.c. conductivity of the iron–bismuth oxide glasses—I

B. K. Chaudhuri, K. Chaudhuri and K. K. Som 1149 Concentration and frequency dependences of a.c. conductivity and dielectric constant of iron–bismuth oxide glasses—II

Oxyfluorides

Zuo-Guang Ye, Régnault Von Der Mühll et Jean Ravez 809 New oxyfluorides and highly densified ceramics related to $LiNbO_3$

Oxygen

Kozo Ishizaki and Koji Watari 1009 Oxygen behavior of normal and HIP sintered AlN

Pairwise interactions

C. Ko and Rex B. McLellan 619 Thermodynamics of C–N austenites

Percolation

R. M. Mostovoy, V. Ya. Sukharev, V. I. Berendyayev, B. V. Kotov and I. A. Myasnikov 541 Structural chemical characteristics and electroconduction mechanism of polymeric ion-radical TCNQ salts based on aliphatic ionenes

Perovskite compounds

P. S. R. Prasad and H. D. Bist 1033 Vibrational spectroscopic study of the structural phase transitions in perovskite layer compounds $(CH_3NH_3)_2\ CdCl_4$

Phase transitions

Hitoshi Kawaji, Tooru Atake and Yasutoshi Saito 215 Heat capacities, magnetic phase transition at 42.02 K and order–disorder phase transition at 673 K of $AgCrS_2$

Keishi Negita and Hiroshi Takao 325 Condensations of phonons at the tetragonal to monoclinic phase transition in ZrO_2

K. Chhor, L. Abello and C. Pommier 423 Low temperature calorimetric and Raman spectrometric studies on lithium ammonium sulphate, $LiNH_4SO_4$

R. A. Dalterio and F. J. Owens 739 Raman study of high pressure induced phase transition in sodium nitrite

Mari Fukai, Takasuke Matsuo and Hiroshi Suga 743 Calorimetric study of phase transitions in ammonium hydrogen oxalate hemihydrate and its deuterated compound

Steven J. Duclos, A. Jayaraman, G. P. Espinosa, A. S. Cooper and R. G. Maines, Sr 769 Raman and optical absorption studies of the pressure-induced zircon to scheelite structure transformation in $TbVO_4$ and $DyVO_4$

N. B. Chanh, J. R. Housty, A. Meresse, L. Ricard and M. Rey-Lafon 829 Polymorphism in the bidimensional compound $(n\text{-}C_{16}H_{33}NH_3)_2CdCl_4$

P. S. R. Prasad and H. D. Bist 1033 Vibrational spectroscopic study of the structural phase transitions in perovskite layer compounds $(CH_3NH_3)_2CdCl_4$

Murray H. Brooker and J. G. Shapter 1087 Raman studies of the phase transition in $KClO_3$

Biswanath Mallik and Ashis Bhattacharjee 1113 Adsorption-induced unusual changes in the electrical conductivity of ferrocene

Syuji Kawada 1177 Acceleration of dielectric relaxation by KOH-doping and phase transition in ice Ih

M. Faucher, D. Garcia, E. Antic-Fidancev and M. Lemaitre-Blaise 1227 The spectrum of Nd^{3+} in rare earth orthoaluminates. The trigonal to orthorhombic transition study of the $^2H_{11/2}$ level

Y. A. Badr and S. B. El-Guiziri 1261 Effect of γ-radiation on the phase transition temperature of $Li_{0.5}(NH_4)_{0.5}SO_4$

J. Zaleski, T. Glowiak, R. Jakbus and L. Sobczyk 1265 Crystal structure and phase transitions of $[(C_2H_5)_4N]_6Bi_8Cl_{30}$

N. Okamoto, M. Oguni and H. Suga 1285 Calorimetric study of thiophene–benzene solutions(I)

Phonons

G. L. Hua, T. R. Welberry and R. L. Withers 207 Lattice dynamics of α- and β-cristobalite, SiO_2

C. Ecolivet, A. Miniewicz and M. Sanquer 651 Elastic constants determination in piezoelectric CT complex of carbazole-1,3,5-trinitrobenzene by Brillouin scattering technique

Joanne R. Rollo and Gary R. Burns 753 Temperature dependences of the Raman spectra of the tetraphosphorus triselenodiiodides (α'-$P_4Se_3I_2$ and β-$P_4Se_3I_2$) and the tetraphosphorus trithiodiiodides (α-$P_4S_3I_2$ and β-$P_4S_3I_2$)

H. C. Gupta, Geeta Sood, Arvind Parashar and B. B. Tripathi 925 Long wavelength optical lattice vibrations in mixed chalcogenide spinels $Zn_{1-x}Cd_xCr_2S_4$ and $CdCr_2(S_{1-x}Se_x)_4$

Keishi Negita and Hiroshi Takao 325 Condensations of phonons at the tetragonal to monoclinic phase transition in ZrO_2

Phosphorescence

A. Halperin 407 The low temperature phosphorescence and thermoluminescence of X-rayed Ge-doped quartz

Z. Burshtein and J. Ivri 1271 Davydov splitting and two-photon excitation of cadmium tungstate ($CsWO_4$) single crystal phosphorescence

Phosphorus

R. A. Nissan and T. A. Vanderah 347 ^{31}P solid state NMR studies of ZrP, Mg_3P_2, MgP_4 and $CdPS_3$

Joanne R. Rollo and Gary R. Burns 399 The temperature and pressure dependence of the Raman spectrum of crystalline tetraphosphorus decasulphide

Photoconductivity

N. V. Joshi, J. C. Sanchez and J. M. Martin 629 Photoconducting properties of InP:Fe

A. C. Pavão and J. P. B. da Silva 669 Electronic structure and charge-transfer transitions in $(NiF_6)^{4-}$

Photoelastic effect

W. Kucharczyk 709 Photoelastic effect and density derivative of the refractive index in alkali halides

Photoemission spectra

Eric Sandré, Raymond Brec and Jean Rouxel 801 Electronic structure of MX_2-type layered compounds

Physisorption

Biswanath Mallik and Ashis Bhattacharjee 1113 Adsorption-induced unusual changes in the electrical conductivity of ferrocene

Polarizability

P. M. Parashak, K. D. Bostic, D. R. Hicks, S. M. Jenkins, John J. Fontanella, Mary C. Wintersgill and C. G. Andeen 867 Effect of pressure on the dielectric constant of arsenic trisulfide glass

Polarization method

Ruben A. Montani and Julio C. Bazán 1207 On the potential range of applicability of Wagner's polarization method

Polarons

M. A. K. L. Dissanayake, O. A. Ileperuma and P. A. G. D. Dharmasena — 359 — A.C. conductivity of $MnWO_4$

B. K. Chaudhuri, K. Chaudhuri and K. K. Som — 1137 — Concentration dependences of d.c. conductivity of the iron–bismuth oxide glasses—I

Polyacetylene

A. Morin, M. Bénierè and F. Bénierè — 611 — Diffusion of $FeCl_4$ in polyacetylene

Polyaniline tetrafluoroborates

Kyung Moon Choi, Keu Hong Kim and Jae Shi Choi — 283 — The chemical and physical properties of electrochemically prepared polyaniline tetrafluoroborates (PATFB)

Polyimide

H. R. Ries, W. L. Harries, S. A. T. Long and E. R. Long, Jr — 735 — Mechanism of electrical conductivity in an irradiated polyimide

Polymers

H. R. Ries, W. L. Harries, S. A. T. Long and E. R. Long, Jr — 735 — Mechanism of electrical conductivity in an irradiated polyimide

Polytypes

Eric Sandré, Raymond Brec and Jean Rouxel — 801 — Electronic structure of MX_2-type layered compounds

Polyvinylchloride–magnetite composites

Jong Ho Jun, Sung Han Lee, Keu Hong Kim and Jae Shi Choi — 785 — Electron transport in polyvinylchloride–magnetite composites

Poole–Frenkel effect

S. R. Dhariwal and P. T. Landsberg — 363 — A theoretical study of field-enhanced emission (Poole–Frenkel effect)

Pore size

Miki Niwa and Yuichi Murakami — 487 — CVD zeolites with controlled pore-opening size

Potassium hydroxide

Rachel Howe and R. W. Whitworth — 963 — The electrical conductivity of KOH-doped ice from 70 to 250 K

Syuji Kawada — 1177 — Acceleration of dielectric relaxation by KOH-doping and phase transition in ice Ih

Potassium–iron–fluoride monohydrate

L. Takács and W. M. Reiff — 33 — Three-dimensional magnetic ordering of $K_2FeF_5 \cdot H_2O$: Mössbauer spectroscopy investigation in the helium-3 temperature range

Precipitation

Gabriel Jasiolek, Zbigniew Golacki and Marek Godlewski — 277 — X-ray characterization of precipitates in HgTe:Eu and ZnS:Eu crystals

Yoshimi Watanabe, A. Sato and T. Mura — 957 — Growth of a nitrogen defect cluster in a bcc lattice examined by a lattice theory

D. Sundararaman, S. Raju and V. S. Raghunathan — 1101 — Theoretical analysis of interstitial ordering and precipitation processes in the Ti–N system

Pressure derivatives

J. Freund and R. Ingalls — 263 — Inverted isothermal equations of state and determination of B_0, B_0' and B_0''

Proton conduction

P. Rajagopal, G. Aruldhas and V. Ramakrishnan — 675 — Raman spectroscopic investigations on the proton conduction in $(NH_4)_3H(SO_4)_2$

Proton mobility

Karin Larsson, Jörgen Tegenfeldt and **Åke Kvick** 107 NMR study of the motion of water molecules in the natural zeolite bikitaite

Pseudoelasticity

E. D. Belokolos and **A. Yu. Gaevsky** 1199 The axial Ising model for martensitic transformations and pseudoelasticity

Pulse-superposition techniques

Richard Barber, Micah Downing, James B. Shaw and **L. S. Cain** 1077 The second-order elastic constants of AgBr–AgCl mixed crystals from 77 to 300 K

Pyroelectricity

R. Poprawski and **A. Kolarz** 693 Thermally stimulated light emission from the linear pyroelectric and ferroelectric surfaces

Quadrupole interactions

M. J. Ponnambalam 273 Effects of cubically symmetric electron density on the electric field gradient in cubic metal alloys

Sushil K. Misra, Kingsley Mbaebie and **S. Subramanian** 1157 Doublet separations of forbidden-hyperfine transitions in the EPR of transition-metal complexes

Quantum size effect

H. T. Chu 319 Eigen energies and eigen states of conduction electrons in pure bismuth under size and magnetic field quantizations

Quantum well structures

Yuan-Ping Feng, Zhilan Huang and **Harold N. Spector** 117 Ionization cross section of excitons due to scattering by free carriers in semiconducting quantum well structures

Quartz

A. Halperin 407 The low temperature phosphorescence and thermoluminescence of X-rayed Ge-doped quartz

Quasimolecular dynamics

Donald Greenspan 1245 Supercomputer simulation of cracks and fractures by quasimolecular dynamics

Radiation effects

D. F. Mariani and **M. Jiménez de Castro** 125 Thermoluminescent processes in Al_2O_3 X-irradiated at 80 K

A. Halperin 407 The low temperature phosphorescence and thermoluminescence of X-rayed Ge-doped quartz

T. Miki, M. R. Hantehzadeh and **L. E. Halliburton** 1003 A new trapped-hole center in irradiated $LiNbO_3$

Raman spectroscopy

Joanne R. Rollo and **Gary R. Burns** 399 The temperature and pressure dependence of the Raman spectrum of crystalline tetraphosphorus decasulphide

K. Chhor, L. Abello and **C. Pommier** 423 Low temperature calorimetric and Raman spectrometric studies on lithium ammonium sulphate, $LiNH_4SO_4$

P. Rajagopal. G. Aruldhas and **V. Ramakrishnan** 675 Raman spectroscopic investigations on the proton conduction in $(NH_4)_3H(SO_4)_2$

R. A. Dalterio and **F. J. Owens** 739 Raman study of high pressure induced phase transition in sodium nitrite

Joanne R. Rollo and **Gary R. Burns** 753 Temperature dependences of the Raman spectra of the tetraphosphorus triselenodiiodides (α'-$P_4Se_3I_2$ and β-$P_4Se_3I_2$) and the tetraphosphorus trithiodiiodides (α-$P_4S_3I_2$ and β-$P_4S_3I_2$)

Steven J. Duclos, A. Jayaraman, G. P. Espinosa, A. S. Cooper and **R. G. Maines, Sr** 769 Raman and optical absorption studies of the pressure-induced zircon to scheelite structure transformation in $TbVO_4$ and $DyVO_4$

M. M. Vergara, E. L. Varetti, G. Rigotti and A. Navaza 951 The crystalline and molecular structure and the vibrational spectra of anhydrous cesium nitroprusside

P. S. R. Prasad and H. D. Bist 1033 Vibrational spectroscopic study of the structural phase transitions in perovskite layer compounds $(CH_3NH_3)_2CdCl_4$

Murray H. Brooker and J. G. Shapter 1087 Raman studies of the phase transition in $KClO_3$

Z. Burshtein, D. O. Henderson, S. Morgan and E. Silberman 1095 Vibrational spectra of chrysoberyl ($BeAl_2O_4$)

Rare earth compounds

B. C. Joshi and U. C. Pandey 599 Interaction between Tb^{3+} and Er^{3+} ions in phosphate glass

F. Fernández, R. Sáez-Puche, C. Cascales, C. M. Marcano and I. Rasines 871 X-ray diffraction data and magnetic properties of the oxides $R_3Sb_5O_{12}$(R = Pr, Nd, Sm, Eu, Gd, Yb)

M. Faucher, D. Garcia, E. Antic-Fidancev and M. Lemaitre-Blaise 1227 The spectrum of Nd^{3+} in rare earth orthoaluminates. The trigonal to orthorhombic transition study of the $^2H_{11/2}$ level

Reflectance spectra

Jamila Ghamri, Hervé Baussart, Michel Le Bras and Jean-Marie Leroy 1237 Spectroscopic study of $Bi_xEu_{1-x}VO_4$ and $Bi_yGd_{1-y}VO_4$ mixed oxides

Refractive index

W. Kucharczyk 233 Ionic sizes in crystals as related to refractive index data

W. Kucharczyk 709 Photoelastic effect and density derivative of the refractive index in alkali halides

Regular solution

D. du Plessis and G. N. van Wyk 237 A model for surface segregation in multicomponent alloys—Part III: the kinetics of surface segregation in a binary alloy

D. du Plessis and G. N. van Wyk 247 A model for surface segregation in multicomponent alloys—Part IV: the kinetics of desegregation in a binary alloy

D. du Plessis and G. N. van Wyk 251 A model for surface segregation in multicomponent alloys—Part V: the kinetics of surface segregation in multicomponent alloys

Relaxation

Partho Sarkar and Patrick S. Nicholson 197 Electric field relaxation studies in the CeO_2–Y_2O_3 system

Peter Adler, Harmut Spiering and Philipp Gutlich 587 Thermodynamics and kinetics of spin state conversion processes studied by pressure dependent Mössbauer spectroscopy

Rocksalt compounds

V. Kumar and G. M. Prasad 899 Electronic properties of ionic rocksalt crystals

Ruthenium dioxide

E. H. P. Cordfunke, R. J. M. Konings, E. F. Westrum, Jr and R. Shaviv 429 The thermophysical and thermochemical properties of RuO_2 from 0 to 1000 K

Saponite

Tadashi Endo, Nobuyuki Nakada, Tsugio Sato and Masahiko Shimada 133 The fluorescence properties of coumarine dye intercalated in a swelling clay

Scandium borate

G. Blasse, J. P. M. van Vliet, J. W. M. Verwey, R. Hoogendam and M. Wiegel 583 Luminescence of Pr^{3+} in scandium borate ($ScBO_3$) and the host lattice dependence of the Stokes shift

Schottky anomaly

Masanori Yoshikawa, Michio Sorai and Hiroshi Suga 713 Heat capacity of a five-coordinated iron(III) complex with spin $S = 3/2$, bromobis (*N*,*N*-dimethyldithiocarbamato) iron(III), between 0.4 and 300 K: new finding of a magnetic phase transition

Schottky formation volume

V. Hadjicontis, K. Eftaxias and C. Varotsos 1193 Connection between the Birch equation of state and the Schottky formation volume in NaCl

Selenium

J. C. Bernede, G. Safoula, R. Messoussi, A. Bonnet and A. Conan 1169 Electrical properties of iodine-doped selenium films

Self-energy

C. L. Roy 111 Relativistic electronic states of disordered systems

Semiconductor properties

Gabriel Jasiolek, Zbigniew Golacki and Marek Godlewski 277 X-ray characterization of precipitates in HgTe:Eu and ZnS:Eu crystals

A. M. Elkorashy 893 Temperature dependence of the optical energy gap in tin monoselenide single crystals

V. Kumar and G. M. Prasad 899 Electronic properties of ionic rocksalt crystals

A. Marbeuf, D. Ballutaud, R. Triboulet, H. Dexpert, P. Lagarde and Y. Marfaing 975 EXAFS and XPS studies of $Hg_{1-x}Zn_xTe$: determination of local atomic structure and valence band maximum

Biswanath Mallik and Ashis Bhattacharjee 1113 Adsorption-induced unusual changes in the electrical conductivity of ferrocene

B. K. Chaudhuri, K. Chaudhuri and K. K. Som 1137 Concentration dependences of d.c. conductivity of the iron–bismuth oxide glasses—I

P. P. Lottici, G. Antonioli and C. Razzetti 967 Ordered-vacancy compound semiconductors: an EXAFS study of the structure of α-$CdIn_2Se_4$

Shear moduli

Pramila Sisodia and M. P. Verma 223 Shear moduli of polycrystalline cubic elements

Silicates

S. K. Saxena and J. Zhang 723 Assessed high-temperature thermochemical data on some solids

Silicon

S. K. Sharma, B. C. Chakravarty, S. N. Singh, B. K. Das, D. C. Parashar, J. Rai and Prabhat K. Gupta 679 Kinetics of growth of thin anodic oxides of silicon at constant voltages

Silver

L. Badrour, E. G. Moya, J. Bernardini and F. Moya 551 Fast diffusion of silver in single and polycrystals of α-alumina

Silver halides

Laura E. Fasano and Julio C. Bazán 259 A theoretical model for silver ion transfer through the solid–solid Ag/AgI interface

R. C. Baetzold, C. R. A. Catlow, J. Corish, F. M. Healy, P. W. M. Jacobs, M. Leslie and Y. T. Tan 791 The effects of three-body interactions on crystal properties and defect energies in silver halides

Richard Barber, Micah Downing, James B. Shaw and L. S. Cain 1077 The second-order elastic constants of AgBr–AgCl mixed crystals from 77 to 300 K

Single crystals

A. M. Elkorashy 893 Temperature dependence of the optical energy gap in tin monoselenide single crystals

Sodium nitrite

R. A. Dalterio and F. J. Owens 739 Raman study of high pressure induced phase transition in sodium nitrite

Soft modes

Mari Fukai, Takasuke Matsuo and Hiroshi Suga — 743 — Calorimetric study of phase transitions in ammonium hydrogen oxalate hemihydrate and its deuterated compound

Solid ammonia

Jens W. Otto, Richard F. Porter and Arthur L. Ruoff — 171 — Equation of state of solid ammonia (NH_3) to 56 GPa

Solid electrolytes

Laura E. Fasano and Julio C. Bazán — 259 — A theoretical model for silver ion transfer through the solid–solid Ag/AgI interface

Rubin A. Montani and Julio C. Bazán — 1207 — On the potential range of applicability of Wagner's polarization method

Solid solutions

Rex B. McLellan — 49 — The thermodynamics of hybrid binary interstitial—substitutional solid solutions

H. Fjellvåg, A. Kjekshus, R. Zach and A. Zięba — 187 — $Mn_{1-t}(Ti_{0.50}V_{0.50})_tAs$; diluted manganese monoarsenide with zero overall chemical pressure

J. L. Baudour, M. M. Granger, L. Toupet, R. Granger and R. Triboulet — 309 — Composition dependence of thermal vibrations in $Hg_{1-x}Zn_xTe$ solid solutions determined by X-ray diffraction

Don Kim, Kyung Moon Choi, Keu Hong Kim and Jae Shi Choi — 821 — Electrical conductivity of the solid solutions $X\,Tm_2O_3 + (1-x)ThO_2$; $0.01 \leqslant X \leqslant 0.15$

A. Taïtai and J. L. Lacout — 851 — On the coupled introduction of Eu^{3+} and S^{2-} ions into strontium apatites

Jong Sik Park, Kyung Moon Choi, Keu Hong Kim and Jae Shi Choi — 909 — Electrical conductivity of the solid solutions $X\,ThO_2 + (1-X)Ho_2O_3$; $0.02 \leqslant X \leqslant 0.10$

F. Picard-Lagnel, B. Poumellec and R. Cortes — 1211 — Study of amorphous thin films of (Ti, Nb)O_2 solid solutions by X-ray absorption at the Ti K edge

N. Okamoto, M. Oguni and H. Suga — 1285 — Calorimetric study of thiophene–benzene solutions(I)

Sound velocity

C. Ecolivet, A. Miniewicz and M. Sanquer — 651 — Elastic constants determination in piezoelectric CT complex of carbazole-1,3,5-trinitrobenzene by Brillouin scattering technique

Space charge

Z. Burshtein — 333 — Comment on "space charge limited current (SCLC) in alkali halide crystals during electrolytic coloration"

Spin correlations

T. H. Kwon — 1083 — Dynamical spin correlations in the Oguchi antiferromagnet

Spin slips

S. Kawano — 633 — Neutron diffraction study of hcp erbium–lanthanum alloys

Spin-crossover

Peter Adler, Harmut Spiering and Philipp Gütlich — 587 — Thermodynamics and kinetics of spin state conversion processes studied by pressure dependent Mössbauer spectroscopy

Spin flop behavior

L. Takács and W. M. Reiff — 33 — Three-dimensional magnetic ordering of $K_2FeF_5 \cdot H_2O$: Mössbauer spectroscopy investigation in the helium-3 temperature range

Spinel compounds

E. Agostinelli, C. Battistoni, D. Fiorani, G. Mattogno and M. Nogues — 269 — An XPS study of the electronic structure of the $Zn_xCd_{1-x}Cr_2X_4$ (X = S, Se) spinel system

H. C. Gupta, Geeta Sood, Arvind Parashar and B. B. Tripathi — 925 — Long wavelength optical lattice vibrations in mixed chalcogenide spinels $Zn_{1-x}Cd_xCr_2S_4$ and $CdCr_2(S_{1-x}Se_x)_4$

Statistical mechanics

Sheikh A. Akbar and Hiroshi Sato 729 Demixing: a source of material deterioration

Stokes shift

G. Blasse, J. P. M. van Vliet, J. W. M. Verwey, R. Hoogendam and M. Wiegel 583 Luminescence of Pr^{3+} in scandium borate ($ScBO_3$) and the host lattice dependence of the Stokes shift

H. Donker, W. M. A. Smit and G. Blasse 603 On the luminescence of Te^{4+} in A_2ZrCl_6 (A = Cs, Rb) and A_2SnCl_6 (A = Cs, Rb, K)

Strain polarizability

W. Kucharczyk 709 Photoelastic effect and density derivative of the refractive index in alkali halides

Strain wave

A. F. Jankowski 641 The strain wave approach to modulus enhancement and stability of metallic multilayers

Strontium compounds

R. Stoyanova, S. Angelov and R. Dafinova 95 Identification of the center of self-activated luminescence in strontium carbonate by doping with lithium

A. Taitai and J. L. Lacout 851 On the coupled introduction of Eu^{3+} and S^{2-} ions into strontium apatites

Structural characterization

K. R. Udayakumar and A. N. Cormack 55 Non-stoichiometry in alkaline earth excess alkaline earth titanates

J. M. Thomas and D. E. W. Vaughan 449 Methodologies to establish the structure and composition of new zeolitic molecular sieves

F. Fernández, R. Sáez-Puche, C. Cascales, C. M. Marcano and I. Rasines 871 X-ray diffraction data and magnetic properties of the oxides $R_3Sb_5O_{12}$ (R = Pr, Nd, Sm, Eu, Gd, Yb)

Superconductivity

H. Verweij and W. H. Bruggink 75 Constant stoichiometry cooling of $YBa_2Cu_3O_x$

Michael M. Rigney, Charles P. Poole, Jr and H. A. Farach 9 Average copper charge and valence states of superconducting copper-oxides

F. Steglech 225 Heavy fermions

Shoichi Nagata, Hiroki Kutsuzawa, Shuji Ebisu, Hidemi Yamamura and Satoshi Taniguchi 703 Superconductivity in the quasi-one-dimensional conductor $TaSe_3$

Shinichi Ichikawa 931 Superconductivity and optimum electronegativity

Superionic conductivity

A. F. Privalov, H.-M. Vieth and I. V. Murin 395 Ionic motion in the LaF_3 superionic conductor studied by ^{19}F NMR with homonuclear decoupling

Superstructures

D. Sundararaman, S. Raju and V. S. Raghunathan 1101 Theoretical analysis of interstitial ordering and precipitation processes in the Ti–N system

Surface charge

Jozef J. Van Dun, Kristine Dhaeze, Wilfried J. Mortier and David E. W. Vaughan 469 The influence of isomorphous substitution on the cation distribution in faujasite-type zeolites; the structures of dehydrated Na-LZ210 and hydrated KGaY

Surface plasmons

J. R. Sambles 1 Optical excitation of surface plasmons

Surface segregation

D. du Plessis and G. N. van Wyk 237 A model for surface segregation in multicomponent alloys—Part III: the kinetics of surface segregation in a binary alloy

D. du Plessis and G. N. van Wyk 247 A model for surface segregation in multicomponent alloys—Part IV: the kinetics of desegregation in a binary alloy

D. du Plessis and G. N. van Wyk 251 A model for surface segregation in multicomponent alloys—Part V: the kinetics of surface segregation in multicomponent alloys

Surface states

Jong Ho Jun, Sung Han Lee, Keu Hong Kim and Jae Shi Choi 785 Electron transport in polyvinylchloride–magnetite composites

Surface tension

D. du Plessis and G. N. van Wyk 237 A model for surface segregation in multicomponent alloys—Part III: the kinetics of surface segregation in a binary alloy

D. du Plessis and G. N. Van Wyk 247 A model for surface segregation in multicomponent alloys—Part IV: the kinetics of desegregation in a binary alloy

D. du Plessis and G. N. van Wyk 251 A model for surface segregation in multicomponent alloys—Part V: the kinetics of surface segregation in multicomponent alloys

Synchrotron radiation

Jens W. Otto, Richard F. Porter and Arthur L. Ruoff 171 Equation of state of solid ammonia (NH_3) to 56 GPa

J. M. Thomas and D. E. W. Vaughan 449 Methodologies to establish the structure and composition of new zeolitic molecular sieves

Szigeti charge

A. K. Koh 39 Systematic variation of the Szigeti charge in the alkali halides with NaCl structure

Thallium compounds

D. Welz, P. Deppe, W. Schaefer, H. Sabrowsky and M. Rosenberg 297 Magnetism of iron–sulfur tetrahedral frameworks in compounds with thallium. I. Chain structures

Thermal conductivity

S. Fujita, A. Garcia, D. O'Leyar, S. Watanabe and T. Burnett 27 On the conductance of a lattice-like network

H. Kaibe, Y. Tanaka, M. Sakata and I. Nishida 945 Anisotropic galvanomagnetic and thermoelectric properties of *n*-type Bi_2Te_3 single crystal with the composition of a useful thermoelectric cooling material

Thermal decomposition

R. Stoyanova, S. Angelov and R. Dafinova 95 Identification of the center of self-activated luminescence in strontium carbonate by doping with lithium

Thermal expansion

S. K. Saxena and J. Zhang 723 Assessed high-temperature thermochemical data on some solids

Thermal vibrations

J. L. Baudour, M. M. Granger, L. Toupet, R. Granger and R. Triboulet 309 Composition dependence of thermal vibrations in $Hg_{1-x}Zn_xTe$ solid solutions determined by X-ray diffraction

Thermodynamics

C. Picard and P. Gerdanian 383 Thermodynamics of $Co_{1-\delta}O$

E. H. P. Cordfunke, R. J. M. Konings, E. F. Westrum, Jr and R. Shaviv 429 The thermophysical and thermochemical properties of RuO_2 from 0 to 1000 K

C. Ko and Rex B. McLellan 619 Thermodynamics of C–N austenites

Regina Krachler, Herbert Ipser and Kurt L. Komarek 1127 Thermodynamics of intermetallic B2-phases. A generalized model

S. H. Lim, G. E. Murch and W. A. Oates 1251 Thermodynamic properties of ternary alloys from Monte Carlo simulations

Thermoelectric properties

H. Kaibe, Y. Tanaka, M. Sakata and I. Nishida 945 Anisotropic galvanomagnetic and thermoelectric properties of *n*-type Bi_2Te_3 single crystal with the composition of a useful thermoelectric cooling material

J. C. Bernede, G. Safoula, R. Messoussi, A. Bonnet and A. Conan 1169 Electrical properties of iodine-doped selenium films

Thermogravimetry

H. Verweij and W. H. M. Bruggink 75 Constant stoichiometry cooling of $YBa_2Cu_3O_x$

Thermoluminescence

D. F. Mariani and M. Jiménez de Castro 125 Thermoluminescent processes in Al_2O_3 X-irradiated at 80 K

A. Halperin 407 The low temperature phosphorescence and thermoluminescence of X-rayed Ge-doped quartz

Thermophysics

E. H. P. Cordfunke, R. J. M. Konings, E. F. Westrum, Jr and R. Shaviv 429 The thermophysical and thermochemical properties of RuO_2 from 0 to 1000 K

Thin films

H. T. Chu and Yimin Ji 1121 Electron transport phenomena in two-dimensional thin films of pure bismuth

J. C. Bernede, G. Safoula, R. Messoussi, A. Bonnet and A. Conan 1169 Electrical properties of iodine-doped selenium films

F. Picard-Lagnel, B. Poumellec and R. Cortes 1211 Study of amorphous thin films of $(Ti,Nb)O_2$ solid solutions by X-ray absorption at the Ti K edge

Melih Öğmen and Walter W. Duley 1221 Excimer laser deposition of thin amorphous carbon films

Thiophene–benzene solutions

N. Okamoto, M. Oguni and H. Suga 1285 Calorimetric study of thiophene–benzene solutions(I)

Three-body interactions

R. C. Baetzold, C. R. A. Catlow, J. Corish, F. M. Healy, P. W. M. Jacobs, M. Leslie and Y. T. Tan 791 The effects of three-body interactions on crystal properties and defect energies in silver halides

Tin monoselenide

A. M. Elkorashy 893 Temperature dependence of the optical energy gap in tin monoselenide single crystals

Titanium compounds

D. Sundararaman, S. Raju and V. S. Raghunathan 1101 Theoretical analysis of interstitial ordering and precipitation processes in the Ti–N system

F. Picard-Lagnel, B. Poumellec and R. Cortes 1211 Study of amorphous thin films of $(Ti,Nb)O_2$ solid solutions by X-ray absorption at the Ti K edge

Topotactic reaction

François Mathieu and Abel Rousset 61 Study of the $\gamma \rightarrow \alpha$ transformation occurring in finely divided γ-Fe_2O_3 in the presence of water and under high pressure (viz. 5.5 GPa)—mechanism of oxyhydroxides formation

Transition-metal compounds

Chikara Sugiura, Michihide Kitamura and Shinji Muramatsu 1069 Chlorine Kβ X-ray emission spectra from selected transition-metal complex compounds

Tri-glycine sulfate (TGS)

R. Poprawski and A. Kolarz 693 Thermally stimulated light emission from the linear pyroelectric and ferroelectric surfaces

Two-dimensional lattices

J. L. Hock and R. B. McQuistan 1051 Constant coverage configurational heat capacities for two-dimensional square-cell lattices

Two-photon absorption

Z. Burshtein and J. Ivri 1271 Davydov splitting and two-photon excitation of cadmium tungstate ($CsWO_4$) single crystal phosphorescence

Urea

El-Metwally Nour and Maha Jobor Al Thani 183 Preparation and infrared spectra of $(Cu(O)(H_2O)_3)$ and $(Cu_2(O)(Cl)_2(H_2O)_2)$ complexes formed in the reactions of Cu(II) salts with urea

V-centres

D. Mariani and M. Jiménez de Castro 125 Thermoluminescent processes in Al_2O_3 X-irradiated at 80 K

Vacancies

J. Misiewicz 1013 Optical and electrical investigations of imperfection levels in Zn_3P_2

P. P. Lottici, G. Antonioli and C. Razzetti 967 Ordered-vacancy compound semiconductors: an EXAFS study of the structure of α-$CdIn_2Se_4$

Valence band structure

Tery L. Barr and Ying Li Liu 657 An X-ray photoelectron spectroscopic study of the valence band structure of indium oxides

Valence states

Micheal M. Rigney, Charles P. Poole, Jr and H. A. Farach 9 Average copper charge and valence states of superconducting copper-oxides

Vibrational analysis

N. B. Chanh, J. R. Housty, A. Meresse, L. Ricard and M. Rey-Lafon 829 Polymorphism in the bidimensional compound $(n\text{-}C_{16}H_{33}NH_3)_2CdCl_4$

Vibrational spectra

Z. Burshtein, D. O. Henderson, S. Morgan and E. Silberman 1095 Vibrational spectra of chrysoberyl ($BeAl_2O_4$)

Water

H. Lechert and W. D. Basler 497 Molecular motion in zeolite sorbends, studied by various NMR methods

X-ray absorption

Chikara Sugiura, Michihide Kitamura and Shinji Muramatsu 1069 Chlorine Kβ X-ray emission spectra from selected transition-metal complex compounds

F. Picard-Lagnel, B. Poumellec and R. Cortes 1211 Study of amorphous thin films of $(Ti,Nb)O_2$ solid solutions by X-ray absorption at the Ti K edge

X-ray diffraction

R. Gerardin, H. Aqachmar, I. Nodari, J. F. Brice et O. Evrard 43 Contribution a l'étude du système Lu_2O_3–Mn_2O_3–Fe_2O_3 et caractérisation de deux varietés cristallographiques de $Lu_2Mn_2Fe_2O_9$

Seok Ho Yun, Keu Hong Kim and Jae Shi Choi 291 Defect structure and electrical conductivity of pure and doped lutetium sesquioxides

J. L. Baudour, M. M. Granger, L. Toupet R. Granger and R. Triboulet 309 Composition dependence of thermal vibrations in $Hg_{1-x}Zn_xTe$ solid solutions determined by X-ray diffraction

G. T. Kokotailo and C. A. Fyfe 441 Perspective: Zeolites; unique materials for research and industry

N. B. Chanh, J. R. Housty, A. Meresse, L. Ricard and M. Rey-Lafon 829 Polymorphism in the bidimensional compound $(n\text{-}C_{16}H_{33}NH_3)CdCl_4$

F. Fernández, R. Sáez-Puche, C. Cascales, C. M. Marcano and I. Rasines — 871 — X-ray diffraction data and magnetic properties of the oxides $R_3Sb_5O_{12}$ (R = Pr, Nd, Sm, Eu, Gd, Yb)

J. Swanepoel — 935 — The distorted *trans*-octahedral molecular geometry of iron(II) difluoride tetrahydrate

X-ray photoelectron spectroscopy

Tery L. Barr and Ying Li Liu — 657 — An X-ray photoelectron spectroscopy study of the valence band structure of indium oxides

A. Marbeuf, D. Ballutaud, R. Triboulet, H. Dexpert, P. Lagarde and Y. Marfaing — 975 — EXAFS and XPS studies of $Hg_{1-x}Zn_xTe$: determination of local atomic structure and valence band maximum

X-ray spectroscopy

Yoo Young Kim, Keu Hong Kim and Jae Shi Choi — 903 — Infrared spectra and electrical conductivity of the α-Fe_2O_3–B_2O_3 system

Chikara Sugiura, Michihide Kitamura and Shinji Muramatsu — 1069 — Chlorine Kβ X-ray emission spectra from selected transition-metal complex compounds

Jamila Ghamri, Hervé Baussart, Michel Le Bras and Jean-Marie Leroy — 1237 — Spectroscopic study of $Bi_xEu_{1-x}VO_4$ and $Bi_yGd_{1-y}VO_4$ mixed oxides

Zeolites

Karin Larsson, Jörgen Tegenfeldt and Åke Kvick — 107 — NMR study of the motion of water molecules in the natural zeolite bikitaite

G. T. Kokotailo and C. A. Fyfe — 441 — Perspective: Zeolites; unique materials for research and industry

J. M. Thomas and D. E. W. Vaughan — 449 — Methodologies to establish the structure and composition of new zeolitic molecular sieves

Jozef J. Van Dun, Kristine Dhaeze, Wilfried J. Mortier and David E. W. Vaughan — 469 — The influence of isomorphous substitution on the cation distribution in faujasite-type zeolites; the structures of dehydrated Na-LZ210 and hydrated KGaY

L. Uytterhoeven, W. J. Mortier and P. Geerlings — 479 — Charge distribution and effective electro-negativity of aluminophosphate frameworks: influence of the structure type

Miki Niwa and Yuichi Murakami — 487 — CVD zeolites with controlled pore-opening size

H. Lechert and W. D. Basler — 497 — Molecular motion in zeolite sorbends, studied by various NMR methods

Robert A. Schoonheydt — 523 — Combined ESR–DRS spectroscopies of transition metal ions and metal ion clusters in zeolites

Zinc phosphide

J. Misiewicz — 1013 — Optical and electrical investigations of imperfection levels in Zn_3P_2

CHEMICAL INDEX

AuCd
Regina Krachler, Herbert Ipser and Kurt L. Komarek 1127 Thermodynamics of intermetallic B2-phases. A generalized model

A_2SnCl_6(A = Cs, Rb, K)
H. Donker, W. M. A. Smit and G. Blasse 603 On the luminescence of Te^{4+} in A_2ZrCl_6(A = Cs, Rb) and A_2SnCl_6 (A = Cs, Rb, K)

A_2ZrCl_6(A = Cs, Rb)
H. Donker, W. M. A. Smit and G. Blasse 603 On the luminescence of Te^{4+} in A_2ZrCl_6(A = Cs, Rb) and A_2SnCl_6 (A = Cs, Rb, K)

BaFBr
R. C. Baetzold 915 Atomistic computation of molecular species in alkaline-earth fluorohalide crystals

BaFCl
R. C. Baetzold 915 Atomistic computation of molecular species in alkaline-earth fluorohalide crystals

$BaLa_{1-x}Nd_xGa_3O_7$
W. Ryba-Romanowski, S. Gołąb, J. Hanuza and M. Berkowski 685 Relaxation of the $^4F_{3/2}$ level of Nd^{3+} in $BaLa_{1-x}Nd_xGa_3O_7$

$BaNO_2 \cdot H_2O$
R. Poprawski and A. Kolarz 693 Thermally stimulated light emission from the linear pyroelectric and ferroelectric surfaces

$BaTiO_3$
A. Jovanović, M. Wöhlecke, S. Kapphan, A. Maillard and G. Godefroy 623 Infrared spectroscopy of hydrogen centers in undoped and iron-doped $BaTiO_3$ crystals

$BeAl_2O_4$
Z. Burshtein, D. O. Henderson, S. Morgan and E. Silberman 1095 Vibrational spectra of chrysoberyl ($BeAl_2O_4$)

$Bi_xEu_{1-x}VO_4$
Jamila Ghamri, Herve Baussart, Michel Le Bras and Jean-Marie Leroy 1237 Spectroscopic study of $Bi_xEu_{1-x}VO_4$ and $Bi_yGd_{1-y}VO_4$ mixed oxides

$Bi_yGd_{1-y}VO_4$
Jamila Ghamri, Herve Baussart, Michel Le Bras and Jean-Marie Leroy 1237 Spectroscopic study of $Bi_xEu_{1-x}VO_4$ and $Bi_yGd_{1-y}VO_4$ mixed oxides

Bi_2O_3-Fe_2O_3
B. K. Chaudhuri, K. Chaudhuri and K. K. Som 1137 Concentration dependences of d.c. conductivity of the iron–bismuth oxide glasses—I

Bi_2Te_3
H. Kaibe, Y. Tanaka, M. Sakata and I. Nishida 945 Anisotropic galvanomagnetic and thermoelectric properties of *n*-type Bi_2Te_3 single crystal with the composition of a useful thermoelectric cooling material

$[(C_2H_5)_4N]_6Bi_8Cl_{30}$
J. Zaleski, T. Głowiak, R. Jakbus and L. Sobczyk 1265 Crystal structure and phase transitions of $[(C_2H_5)_4N]_6Bi_8Cl_{30}$

$CaWO_4$:Tb^{3+}
A. G. Page, S. V. Godbole and M. D. Sastry 571 Electronic spectra and co-operative optical transitions in $CaWO_4$:Tb^{3+} single crystal

$(n\text{-}C_{16}H_{33}NH_3)_2CdCl_4$
N. B. Chan, J. R. Housty, A. Meresse, L. Ricard and M. Rey-Lafon — 829 — Polymorphism in the bidimensional compound $(n\text{-}C_{16}H_{33}NH_3)_2CdCl_4$

$Cd(CH_3OO)_2 \cdot 3H_2O : Mn^{2+}$
Sushil K. Misra, Kingsley Mbaebie and S. Subramanian — 1157 — Doublet separations of forbidden-hyperfine transitions in the EPR of transition-metal complexes

$CdC_4H_6O_6 : VO^{2+}$
R. S. Bansal, V. P. Seth and Prem Chand — 839 — EPR study of vanadyl ion in cadmium maleate dihydrate single crystals

$CdCr_2(S_{1-x}Se_x)_4$
H. C. Gupta, Geeta Sood, Arvind Parashar and B. B. Tripathi — 925 — Long wavelength optical lattice vibrations in mixed chalcogenide spinels $Zn_{1-x}Cd_xCr_2S_4$ and $CdCr_2(S_{1-x}Se_x)_4$

$CdGa_2Se_4$
P. P. Lottici, G. Antonioli and C. Razzetti — 967 — Ordered-vacancy compound semiconductors: an EXAFS study of the structure of $\alpha\text{-}CdIn_2Se_4$

$CdIn_2Se_4$
P. P. Lottici, G. Antonioli and C. Razzetti — 967 — Ordered-vacancy compound semiconductors: an EXAFS study of the structure of $\alpha\text{-}CdIn_2Se_4$

$CdPS_3$
R. A. Nissan and T. A. Vanderah — 347 — ^{31}P solid state NMR studies of ZrP, Mg_3P_2, MgP_4 and $CdPS_3$

$CdWO_4$
Z. Burshtein and J. Ivri — 1271 — Davydov splitting and two-photon excitation of cadmium tungstate ($CdWO_4$) single crystal phosphorescence

$Ce_2Co_{12}P_7$
Manfred Reehuis and Wolfgang Jeitschko — 563 — Magnetic properties of lanthanoid iron and cobalt phosphides with $Zr_2Fe_{12}P_7$ type structure

$(CH)_x : FeCl_4$
A. Morin, M. Bénière and F. Bénière — 611 — Diffusion of $FeCl_4^-$ in polyacetylene

$(CH_3NH_3)_2CdCl_4$
P. S. R. Prasad and H. D. Bist — 1033 — Vibrational spectroscopic study of the structural phase transitions in perovskite layer compounds $(CH_3NH_3)_2CdCl_4$

$CoCuSnO_4$
Sangeetha Sampath, R. R. Tripathi and M. P. Tare — 921 — Structural and electrical properties of $CoCuSnO_4$ prepared by two different methods

$Co_{1-\delta}O$
C. Picard and P. Gerdanian — 383 — Thermodynamics of $Co_{1-\delta}O$

CO_2^-
F. Callens, P. Matthys and E. Boesman — 377 — Paramagnetic resonance spectrum of CO_2^- trapped in KCl

CoO–FeO
D. J. Young, F. Viani and F. Gesmundo — 415 — Effect of the deviation from stoichiometry on the activity of pure oxides and of oxide solid solutions

CoO–NiO
D. J. Young, F. Viani and F. Gesmundo — 415 — Effect of the deviation from stoichiometry on the activity of pure oxides and of oxide solid solutions

$Cs_2[Fe(CN)_5NO]$
M. M. Vergara, E. L. Varetti, G. Rigotti and A. Navaza — 951 — The crystalline and molecular structure and the vibrational spectra of anhydrous cesium nitroprusside

Cs_2IrCl_6
John Gilchrist — 857 — Low temperature dielectric relaxations in ammonium hexachlorostannate and some other antifluorites

Cs_2PtBr_6
John Gilchrist — 857 Low temperature dielectric relaxations in ammonium hexachlorostannate and some other antifluorites

Cs_2PtCl_6
John Gilchrist — 857 Low temperature dielectric relaxations in ammonium hexachlorostannate and some other antifluorites

Cs_2SnBr_6
John Gilchrist — 857 Low temperature dielectric relaxations in ammonium hexachlorostannate and some other antifluorites

Cs_2SnCl_6
John Gilchrist — 857 Low temperature dielectric relaxations in ammonium hexachlorostannate and some other antifluorites

$CuCl_2 \cdot 2H_2O$
El-Metwally Nour and Maha Jabor Al Thani — 183 Preparation and infrared spectra of $(Cu(O)(H_2O)_3)$ and $(Cu_2(O)(Cl)_2(H_2O)_2)$ complexes formed in the reactions of Cu(II) salts with urea

$Cu_xCo_{3-x}O_4$
K. Petrov, K. Krezhov and P. Konstantinov — 577 Neutron diffraction study of the cationic distribution in $Cu_xCo_{3-x}O_4 (0 \leq x \leq 1.0)$ spinels prepared by thermal decomposition of layered hydroxide nitrate precursors

$Cu_2(O)(Cl)_2(H_2O)_2$
El-Metwally Nour and Maha Jabor Al Thani — 183 Preparation and infrared spectra of $(Cu(O)(H_2O)_3)$ and $(Cu_2(O)(Cl)_2(H_2O)_2)$ complexes formed in the reactions of Cu(II) salts with urea

$Cu(O)(H_2O)_3$
El-Metwally Nour and Maha Jabor Al Thani — 183 Preparation and infrared spectra of $(Cu(O)(H_2O)_3)$ and $(Cu_2(O)(Cl)_2(H_2O)_2)$ complexes formed in the reactions of Cu(II) salts with urea

$CuInS_2$
H. Y. Ueng and H. L. Hwang — 1297 The defect structure of $CuInS_2$. Part I: intrinsic defects

$CuSO_4 \cdot 5H_2O$
El-Metwally Nour and Maha Jabor Al Thani — 183 Preparation and infrared spectra of $(Cu(O)(H_2O)_3)$ and $(Cu_2(O)(Cl)_2(H_2O)_2)$ complexes formed in the reactions of Cu(II) salts with urea

$CuWO_4$
S. K. Arora, Thomas Mathew and N. M. Batra — 665 Optical characterization of $CuWO_4$ single crystals

$DyVO_4$
Steven J. Duclos, A. Jayaraman, G. P. Espinosa, A. S. Cooper and R. G. Maines, Sr — 769 Raman and optical absorption studies of the pressure-induced zircon to scheelite structure transformation in $TbVO_4$ and $DyVO_4$

Er–La
S. Kawano — 633 Neutron diffraction study of hcp erbium–lanthanum alloys

$Eu_{1.79}TeO_x$
J. P. M. van Vliet and G. Blasse — 1277 Luminescence and energy transfer in europium tellurite anti-glass phases

FeF_2
P. L. Crouse — 369 A conversion electron Mössbauer spectroscopic study of the reactions between hydrogen fluoride and iron oxide surface films in the presence and absence of oxygen and water vapour

$FeF_2 \cdot 4H_2O$
P. L. Crouse — 369 A conversion electron Mössbauer spectroscopic study of the reactions between hydrogen fluoride and iron oxide surface films in the presence and absence of oxygen and water vapour

$FeF_3 \cdot H_2O$
P. L. Crouse — 369 A conversion electron Mössbauer spectroscopic study of the reactions between hydrogen fluoride and iron oxide surface films in the presence and absence of oxygen and water vapour

$Fe_2F_5 \cdot 2H_2O$
P. L. Crouse — 369 A conversion electron Mössbauer spectroscopic study of the reactions between hydrogen fluoride and iron oxide surface films in the presence and absence of oxygen and water vapour

$Fe_{16}N_2$
Yoshimi Watanabe, A. Sato and T. Mura — 957 Growth of a nitrogen defect cluster in a bcc lattice examined by a lattice theory

Fe_2O_3
P. L. Crouse — 369 A conversion electron Mössbauer spectroscopic study of the reactions between hydrogen fluoride and iron oxide surface films in the presence and absence of oxygen and water vapour

γ-Fe_2O_3
Francois Mathieu and Abel Rousset — 61 Study of the $\gamma \rightarrow \alpha$ transformation occurring in finely divided γ-Fe_2O_3 in the presence of water and under high pressure (viz. 5.5 GPa)—mechanism of oxyhydroxides formation

Fe_2O_3–B_2O_3
Yoo Young Kim, Keu Hong Kim and Jae Shi Choi — 903 Infrared spectra and electrical conductivity of the α-Fe_2O_3–B_2O_3 system

$FeF_3 \cdot 3H_2O$
P. L. Crouse — 369 A conversion electron Mössbauer spectroscopic study of the reactions between hydrogen fluoride and iron oxide surface films in the presence and absence of oxygen and water vapour

Fe_2O_3–Bi_2O_3
B. K. Chaudhuri, K. Chaudhuri and K. K. Som — 1137 Concentration dependence of d.c. conductivity of the iron–bismuth oxide glasses—I

$x Fe_2O_3$–$(100-x)Bi_2O_3$
B. K. Chaudhuri, K. Chaudhuri and K. K. Som — 1137 Concentration dependence of d.c. conductivity of the iron–bismuth oxide glasses—I

$x Fe_2O_3$–$(100-x)Bi_2O_3$
B. K. Chaudhuri, K. Chaudhuri and K. K. Som — 1149 Concentration and frequency dependences of a.c. conductivity and dielectric constant of iron–bismuth oxide glasses—II

GaSe
Eric Sandre, Raymond Brec and Jean Rouxel — 801 Electronic structure of MX_2-type layered compounds

$Hg_{1-x}Zn_xTe$
A. Marbeuf, D. Ballutaud, R. Triboulet, H. Dexpert, P. Lagarde and Y. Marfaing — 975 EXAFS and XPS studies of $Hg_{1-x}Zn_xTe$: determination of local atomic structure and valence band maximum

Ho–Ce
S. Kawano and N. Achiwa — 353 Magnetic phase diagram of hcp phases in binary systems between Ho and light rare-earths: La, Ce, Pr

Ho–La
S. Kawano and N. Achiwa — 353 Magnetic phase diagram of hcp phases in binary systems between Ho and light rare-earths: La, Ce, Pr

Ho–Pr
S. Kawano and N. Achiwa — 353 Magnetic phase diagram of hcp phases in binary systems between Ho and light rare-earths: La, Ce, Pr

Ho_2O_3–ThO_2
Jong Sik Park, Kyung Moon Choi, Keu Hong Kim and Jae Shi Choi — 909 Electrical conductivity of the solid solutions $XThO_2 + (1 - X)Ho_2O_3$; $0.02 \leq X \leq 0.10$

InP
N. V. Joshi, J. C. Sanchez and J. M. Martin — 629 Photoconducting properties of InP:Fe

InP:Fe
N. V. Joshi, J. C. Sanchez and J. M. Martin — 629 Photoconducting properties of InP:Fe

K_2IrCl_6
John Gilchrist — 857 Low temperature dielectric relaxations in ammonium hexachlorostannate and some other antifluorites

K_2PtCl_6
John Gilchrist — 857 Low temperature dielectric relaxations in ammonium hexachlorostannate and some other antifluorites

K_2SnBr_6
John Gilchrist — 857 Low temperature dielectric relaxations in ammonium hexachlorostannate and some other antifluorites

K_2SnCl_6
John Gilchrist — 857 Low temperature dielectric relaxations in ammonium hexachlorostannate and some other antifluorites

KCl:CO_2
F. Callens, P. Matthys and E. Boesman — 377 Paramagnetic resonance spectrum of CO_2 trapped in KCl

$KClO_3$
Murray H. Brooker and J. G. Shapter — 1087 Raman studies of the phase transition in $KClO_3$

KF
W. Kucharczyk — 709 Photoelastic effect and density derivative of the refractive index in alkali halides

LaB_3O_6:Gd^{3+}
J. W. M. Verwey, G. F. Imbusch and G. Blasse — 813 Laser excited spectroscopy of Gd^{3+} ions in crystalline and glass borate hosts with comparable composition

$LaBO_3$:Pr^{3+}
G. Blasse, J. P. M. van Vliet, J. W. M. Verwey, R. Hoogendam and M. Wiegel — 583 Luminescence of Pr^{3+} in scandium borate ($ScBO_3$) and the host lattice dependence of the Stokes shift

LaF_3
A. F. Privalov, H.-M. Vieth and I. V. Murin — 395 Ionic motion in the LaF_3 superionic conductor studied by ^{19}F NMR with homonuclear decoupling

$La_{2-2x}Sr_{2x}Ni_{1-x}Fe_xO_{4-(x/2)+\delta}$
R. Benloucif, N. Nguyen, J. M. Greneche and B. Raveau — 435 $La_{2-2x}Sr_{2x}Ni_{1-x}Fe_xO_{4-(x/2)+\delta}$: magnetic and electron transport properties

$Li_{0.5}(NH_4)_{0.5}SO_4$
Y. A. Badr and S. B. El-Guiziri — 1261 Effect of γ-radiation on the phase transition temperature of $Li_{0.5}(NH_4)_{0.5}SO_4$

$LiNH_4SO_4$
K. Chhor, L. Abello and C. Pommier — 423 Low temperature calorimetric and Raman spectrometric studies on lithium ammonium sulphate, $LiNH_4SO_4$

LiCl
W. Kucharczyk — 709 Photoelastic effect and density derivative of the refractive index in alkali halides

$LiF:Be^{2+}$
J. Grammatikakis, C. A. Londos, V. Katsika and N. Bogris 845 Migration enthalpy of the cation vacancies in $LiF:Be^{2+}$

$LiIO_3$
R. Poprawski and A. Kolarz 693 Thermally stimulated light emission from the linear pyroelectric and ferroelectric surfaces

$LiNbO_3$
Zuo-Guang Ye, Régnault Von Der Mühll et Jean Ravez 809 New oxyfluorides and highly densified ceramics related to $LiNbO_3$

$LiNbO_3$
T. Miki, M. R. Hantehzadeh and L. E. Halliburton 1003 A new trapped-hole center in irradiated $LiNbO_3$

$Ln_2Co_{12}P_7$(Ln = lanthanide)
Manfred Reehuis and Wolfgang Jeitschko 563 Magnetic properties of lanthanoid iron and cobalt phosphides with $Zr_2Fe_{12}P_7$ type structure

$Ln_2Fe_{12}P_7$(Ln = lanthanide)
Manfred Reehuis and Wolfgang Jeitschko 563 Magnetic properties of lanthanoid iron and cobalt phosphides with $Zr_2Fe_{12}P_7$ type structure

Mg_3P_2
R. A. Nissan and T. A. Vanderah 347 ^{31}P solid state NMR studies of ZrP, Mg_3P_2, MgP_4 and $CdPS_3$

MgP_4
R. A. Nissan and T. A. Vanderah 347 ^{31}P solid state NMR studies of ZrP, Mg_3P_2, MgP_4 and $CdPS_3$

$MnWO_4$
M. A. K. L. Dissanayake, O. A. Ileperuma and P. A. G. D. Dharmasena 359 A.C. conductivity of $MnWO_4$

$Na_2P_2O_6:Er^{3+}$
B. C. Joshi and U. C. Pandey 599 Interaction between Tb^{3+} and Er^{3+} ions in phosphate glass

$Na_2P_2O_6:Tb^{3+}$
B. C. Joshi and U. C. Pandey 599 Interaction between Tb^{3+} and Er^{3+} ions in phosphate glass

NaBr
W. Kucharczyk 709 Photoelastic effect and density derivative of the refractive index in alkali halides

NaCl
V. Hadjicontis, K. Eftaxias and C. Varotsos 1193 Connection between the Birch equation of state and the Schottky formation volume in NaCl

NaF
W. Kucharczyk 709 Photoelastic effect and density derivative of the refractive index in alkali halides

NaI
W. Kucharczyk 709 Photoelastic effect and density derivative of the refractive index in alkali halides

$Nd_xSm_{1-x}AlO_3$
M. Faucher, D. Garcia, E. Antic-Fidancev and M. Lemaitre-Blaise 1227 The spectrum of Nd^{3+} in rare earth orthoaluminates. The trigonal to orthorhombic transition study of the $^2H_{11/2}$ level

$(NH_4)_2GeF_6$
John Gilchrist 857 Low temperature dielectric relaxations in ammonium hexachlorostannate and some other antifluorites

$(NH_4)_2IrCl_6$
John Gilchrist 857 Low temperature dielectric relaxations in ammonium hexachlorostannate and some other antifluorites

$(NH_4)_2PtBr_6$
John Gilchrist — 857 Low temperature dielectric relaxations in ammonium hexachlorostannate and some other antifluorites

$(NH_4)_2PtCl_6$
John Gilchrist — 857 Low temperature dielectric relaxations in ammonium hexachlorostannate and some other antifluorites

$(NH_4)_2SiF_6$
John Gilchrist — 857 Low temperature dielectric relaxations in ammonium hexachlorostannate and some other antifluorites

$(NH_4)_2SnBr_6$
John Gilchrist — 857 Low temperature dielectric relaxations in ammonium hexachlorostannate and some other antifluorites

$(NH_4)_2SnCl_6$
John Gilchrist — 857 Low temperature dielectric relaxations in ammonium hexachlorostannate and some other antifluorites

$(NH_4)_3H(SO_4)_2$
P. Rajagopal, G. Aruldhas and V. Ramakrishnan — 675 Raman spectroscopic investigations on the proton conduction in $(NH_4)_3H(SO_4)_2$

NH_4HSeO_4
R. Poprawski and A. Kolarz — 693 Thermally stimulated light emission from the linear pyroelectric and ferroelectric surfaces

NiAl
Regina Krachler, Herbert Ipser and Kurt L. Komarek — 1127 Thermodynamics of intermetallic B2-phases. A generalized model

NiF_2
A. C. Pavão and J. P. B. da Silva — 669 Electronic structure and charge-transfer transitions in $(NiF_6)^{4-}$

P_4S_{10}
Joanne R. Rollo and Gary R. Burns — 399 The temperature and pressure dependence of the Raman spectrum of crystalline tetraphosphorus decasulphide

$P_4S_3I_2$
Joanne R. Rollo and Gary R. Burns — 753 Temperature dependences of the Raman spectra of the tetraphosphorus triselenodiiodides (α'-$P_4Se_3I_2$ and β-$P_4Se_3I_2$) and the tetraphosphorus trithiodiiodides (α-$P_4S_3I_2$ and β-$P_4S_3I_2$)

$P_4Se_3I_2$
Joanne R. Rollo and Gary R. Burns — 753 Temperature dependences of the Raman spectra of the tetraphosphorus triselenodiiodides (α'-$P_4Se_3I_2$ and β-$P_4Se_3I_2$) and the tetraphosphorus trithiodiiodides (α-$P_4S_3I_2$ and β-$P_4S_3I_2$)

PdMn
Regina Krachler, Herbert Ipser and Kurt L. Komarek — 1127 Thermodynamics of intermetallic B2-phases. A generalized model

$R_3Sb_5O_{12}$
F. Fernández, R. Sáez-Puche, C. Cascales, C. M. Marcano and I. Rasines — 871 X-ray diffraction data and magnetic properties of the oxides $R_3Sb_5O_{12}$ (R = Pr, Nd, Sm, Eu, Gd, Yb)

Rb_2PtBr_6
John Gilchrist — 857 Low temperature dielectric relaxations in ammonium hexachlorostannate and some other antifluorites

Rb_2SnBr_6
John Gilchrist — 857 Low temperature dielectric relaxations in ammonium hexachlorostannate and some other antifluorites

Rb_2SnCl_6
John Gilchrist — 857 Low temperature dielectric relaxations in ammonium hexachlorostannate and some other antifluorites

RuO_2
E. H. P. Cordfunke, R. J. M. Konings, E. F. Westrum, Jr and R. Shaviv — 429 The thermophysical and thermochemical properties of RuO_2 from 0 to 1000 K

Sb–Te
G. Alonzo, L. Garbato, F. Ledda and C. Muntoni — 1195 121-antimony Mössbauer spectroscopic study on some antimony–tellurium alloys

$ScBO_3:Pr^{3+}$
G. Blasse, J. P. M. van Vliet, J. W. M. Verwey, R. Hoogendam and M. Wiegel — 583 Luminescence of Pr^{3+} in scandium borate ($ScBO_3$) and the host lattice dependence of the Stokes shift

ScC
A. L. Ivanovsky, V. I. Anisimov and V. A. Gubanov — 883 The influence of structural defects on the electronic properties of interstitial alloys—IV. The electronic structure of 3*d*-, 4*d*-metallic impurities in ScC, TiC, VC and ZrC

SiO_2
J. Minge and J. A. Weil — 997 ^{57}Fe hyperfine structure of $[FeO_4/Li]^0$ center in α-quartz

$SiO_2:[FeO_4/Li]^0$
J. Minge and J. A. Weil — 997 ^{57}Fe hyperfine structure of $[FeO_4/Li]^0$ center in α-quartz

$Sr_{10-x}Eu_x(PO_4)_6S_x(0 \leq x \leq 2)$
A. Taitai and J. L. Lacout — 851 On the coupled introduction of Eu^{3+} and S^{2-} ions into strontium apatites

SrFCl
R. C. Baetzold — 915 Atomistic computation of molecular species in alkaline-earth fluorohalide crystals

$SrTiO_3$
J. Ravez, A. Simon, J. P. Bonnet, C. Denage et J. L. Miane — 1041 Propriétés diélectriques en hautes fréquences de céramiques à couches d'arrêt de type $SrTiO_3$

$TaSe_3$
Shoichi Nagata, Hiroki Kutsuzawa, Shuji Ebisu, Hidemi Yamamura and Satoshi Taniguchi — 703 Superconductivity in the quasi-one-dimensional conductor $TaSe_3$

$TbVO_4$
Steven J. Duclos, A. Jayaraman, G. P. Espinosa, A. S. Cooper and R. G. Maines, Sr — 769 Raman and optical absorption studies of the pressure-induced zircon to scheelite structure transformation in $TbVO_4$ and $DyVO_4$

ThO_2–Gd_2O_3
Keu Hong Kim, Do Young Kim, Kyung Moon Choi, Jae Shi Choi and Robert G. Sauer — 1027 Electrical conductivity of the solid solutions $XGd_2O_3 + (1 - X)ThO_2$; $0.01 \leq X \leq 0.12$

ThO_2–Tm_2O_3
Don Kim, Kyung Moon Choi, Keu Hong Kim and Jae Shi Choi — 821 Electrical conductivity of the solid solutions $XTm_2O_3 + (1 - X)ThO_2$; $0.01 \leq X \leq 0.15$

Ti
Rex B. McLellan and Franz R. Brotzen — 1045 The effect of oxygen interstitial doping on "fast" diffusion in α-titanium

TiC
A. L. Ivanovsky, V. I. Anisimov and V. A. Gubanov — 883 The influence of structural defects on the electronic properties of interstitial alloys—IV. The electronic structure of 3*d*-, 4*d*-metallic impurities in ScC, TiC, VC and ZrC

(Ti, Nb)O_2
F. Picard-Lagnel, B. Poumellec and R. Cortes — 1211 Study of amorphous thin films of (Ti, Nb)O_2 solid solutions by X-ray absorption at the Ti K edge

Ti–N
D. Sundararaman, S. Raju and **V. S. Raghunathan** 1101 Theoretical analysis of interstitial ordering and precipitation processes in the Ti–N system

VC
A. L. Ivanovsky, V. I. Anisimov and **V. A. Gubanov** 883 The influence of structural defects on the electronic properties of interstitial alloys—IV. The electronic structure of 3*d*-, 4*d*-metallic impurities in ScC, TiC, VC and ZrC

$YBO_3:Pr^{3+}$
G. Blasse, J. P. M. van Vliet, J. W. M. Verwey, R. Hoogendam and **M. Wiegel** 583 Luminescence of Pr^{3+} in scandium borate ($ScBO_3$) and the host lattice dependence of the Stokes shift

$Zn_{1-x}Cd_xCr_2S_4$
H. C. Gupta, Geeta Sood, Arvind Parashar and **B. B. Tripathi** 925 Long wavelength optical lattice vibrations in mixed chalcogenide spinels $Zn_{1-x}Cd_xCr_2S_4$ and $CdCr_2(S_{1-x}Se_x)_4$

Zn_3P_2
J. Misiewicz 1013 Optical and electrical investigations of imperfection levels in Zn_3P_2

ZrC
A. L. Ivanovsky, V. I. Anisimov and **V. A. Gubanov** 883 The influence of structural defects on the electronic properties of interstitial alloys—IV. The electronic structure of 3*d*-, 4*d*-metallic impurities in ScC, TiC, VC and ZrC

ZrP
R. A. Nissan and **T. A. Vanderah** 347 ^{31}P solid state NMR studies of ZrP, Mg_3P_2, MgP_4 and $CdPS_3$

JOURNAL OF PHYSICS AND CHEMISTRY OF SOLIDS

AIMS & SCOPE

The *Journal of Physics and Chemistry of Solids* is an established international medium for the solid state sciences covering all aspects of the fundamental physics and chemistry of the solid state. Emphasis is placed upon experimental and theoretical work which elucidates the basic properties of and processes in condensed systems. Typical fields of interest are electronic, spectroscopic and structural properties of solids, and the statistical mechanics and thermodynamics of condensed systems. These systems include perfect and defect lattices, surfaces and interfaces, amorphous materials, and layered and low-dimensional structures. Invited topical Review Articles, Perspectives, which are brief invited discussions of new developments, and Special Issues in rapidly developing fields are also published.

NOTES FOR CONTRIBUTORS

I. GENERAL

1. Submission of a paper to the *Journal of Physics and Chemistry of Solids* will be taken to imply that it represents original research not previously published (except in the form of an abstract or preliminary report), that it is not being considered for publication elsewhere, and that if accepted it will not be published elsewhere in the same form, in any language, without the consent of the Editors. It should deal with original research work in the field of the physics and chemistry of solids.

2. Papers may be submitted directly to the editorial office or to the appropriate regional editor.

3. Short communications may be published as "Technical Notes" and will receive somewhat more rapid handling than full length articles. Short communications requiring the maximum speed of publication should be submitted to one of the editors of *Solid State Communications*.

4. Short papers, approximately two journal pages or less in length, may be submitted for the Software Survey Section. These papers should provide a brief description of the purpose and application of the program and its availability. For further details, see the editorial in Volume 46, page 1, or write to the Journal office.

5. *Reprints.* A reprint form will be sent with proofs. Authors will automatically receive 25 free reprints of their article. Any additional reprints may be bought at the rate indicated on the form.

II. SCRIPT REQUIREMENTS

1. **Papers** submitted should be concise and written in a readily understandable style. Scripts should be typed and double spaced with good margins on one side of the paper only and submitted in duplicate to facilitate refereeing.

It will be appreciated if authors clearly indicate any special characters used. An abstract not exceeding 200 words (100 words in the case of a Technical Note or article submitted for the Software Survey Section) should be provided in the language of the paper. French and German papers should be submitted with English abstract and titles, but if this is not possible the abstract will be translated by the publishers. Normally a brief description of experimental techniques and mathematical derivations is adequate; a detailed description should be given only when these are new. Between four to eight appropriate key words should be provided just below the abstract for subsequent use in computer data bases. References to internal reports and doctoral theses should be avoided. Authors will receive proofs for correction when their papers are first set, and **alterations must be restricted to printer's errors.** Other than these, any substantial changes may be charged to authors.

2. **Illustrations** should not be included in the typescript of the paper, and legends should be typed on a separate sheet. Line drawings which require redrawing should include all relevant details and clear instructions for the draughtsman. If figures are already well drawn it may be possible to reproduce them direct from the originals, or from good photo-prints if these can be provided. It is not possible to reproduce from prints with weak lines. Illustrations for reproduction should normally be about twice the final size required. The lettering should be sufficiently large and bold to permit this reduction. Photographs should only be included where they are essential.

3. **Tables and figures** should be so constructed as to be intelligible without reference to the text. Every table and column should be provided with an explanatory heading. Units of measure must always be clearly indicated.

In the interest of economy and in order to avoid the introduction of errors, tables will be reproduced by photo-offset means directly from the author's typed manuscripts. The guidelines detailed below should be followed:
1. Page size should be 8.5 × 11 in. (or 21 × 30 cm). 2. Large or long tables should be typed on continuing sheets. 3. Table headings should be typed on separate sheets but identifying numbers should be placed on the upper righthand corner of each sheet of tabular material. 4. Original typed tables are required. It will be the author's responsibility to prepare his tables in accordance with this procedure as no facilities exist at the Editorial Office for retyping. The same data should not be published in both tables and figures. The following standard symbols should be used on line drawings since they are easily available to the printers: ○●+×□■△▲◇◆▽▼.

4. **References** are indicated in the text by numbers on the line brackets, and the full reference should be given in a list at the end of the paper in the following form:

1. Barnes R. G., Borsa F. and Peteson D., *J. appl. Phys.* **36,** 940 (1965).
2. Knight W. D., *Solid State Physics* (Edited by F. Seitz and D. Turnbull), Vol. 2, p. 93. Academic Press, New York (1957).

Abbreviations of journal titles should follow those given in *World List of Scientific Periodicals* (1979).

Footnotes, as distinct from literature references, should be indicated by the following symbols—†, ‡, §, ¶, ‖, commencing anew on each page; they should *not* be included in the numbered reference system.

5. Due to the international character of the journal no rigid rules concerning notation and spelling will be observed, but each paper should be consistent within itself as to symbols and units.

The original manuscript and diagrams will be discarded one month after publication unless the Publisher is requested to return the original material to the author.

Printed in Great Britain by BPCC Wheatons Ltd, Exeter

JOURNAL OF PHYSICS AND CHEMISTRY OF SOLIDS

AIMS & SCOPE

The *Journal of Physics and Chemistry of Solids* is an established international medium for the solid state sciences covering all aspects of the fundamental physics and chemistry of the solid state. Emphasis is placed upon experimental and theoretical work which elucidates the basic properties of and processes in condensed systems. Typical fields of interest are electronic, spectroscopic and structural properties of solids, and the statistical mechanics and thermodynamics of condensed systems. These systems include perfect and defect lattices, surfaces and interfaces, amorphous materials, and layered and low-dimensional structures. Invited topical Review Articles, Perspectives, which are brief invited discussions of new developments, and Special Issues in rapidly developing fields are also published.

NOTES FOR CONTRIBUTORS

I. GENERAL

1. Submission of a paper to the *Journal of Physics and Chemistry of Solids* will be taken to imply that it represents original research not previously published (except in the form of an abstract or preliminary report), that it is not being considered for publication elsewhere, and that if accepted it will not be published elsewhere in the same form, in any language, without the consent of the Editors. It should deal with original research work in the field of the physics and chemistry of solids.

2. Papers may be submitted directly to the editorial office or to the appropriate regional editor.

3. Short communications may be published as "Technical Notes" and will receive somewhat more rapid handling than full length articles. Short communications requiring the maximum speed of publication should be submitted to one of the editors of *Solid State Communications*.

4. Short papers, approximately two journal pages or less in length, may be submitted for the Software Survey Section. These papers should provide a brief description of the purpose and application of the program and its availability. For further details, see the editorial in Volume 46, page 1, or write to the Journal office.

5. *Reprints.* A reprint form will be sent with proofs. Authors will automatically receive 25 free reprints of their article. Any additional reprints may be bought at the rate indicated on the form.

II. SCRIPT REQUIREMENTS

1. **Papers** submitted should be concise and written in a readily understandable style. Scripts should be typed and double spaced with good margins on one side of the paper only and submitted in duplicate to facilitate refereeing.

It will be appreciated if authors clearly indicate any special characters used. An abstract not exceeding 200 words (100 words in the case of a Technical Note or article submitted for the Software Survey Section) should be provided in the language of the paper. French and German papers should be submitted with English abstract and titles, but if this is not possible the abstract will be translated by the publishers. Normally a brief description of experimental techniques and mathematical derivations is adequate; a detailed description should be given only when these are new. Between four to eight appropriate key words should be provided just below the abstract for subsequent use in computer data bases. References to internal reports and doctoral theses should be avoided. Authors will receive proofs for correction when their papers are first set, and **alterations must be restricted to printer's errors.** Other than these, any substantial changes may be charged to authors.

2. **Illustrations** should not be included in the typescript of the paper, and legends should be typed on a separate sheet. Line drawings which require redrawing should include all relevant details and clear instructions for the draughtsman. If figures are already well drawn it may be possible to reproduce them direct from the originals, or from good photo-prints if these can be provided. It is not possible to reproduce from prints with weak lines. Illustrations for reproduction should normally be about twice the final size required. The lettering should be sufficiently large and bold to permit this reduction. Photographs should only be included where they are essential.

3. **Tables and figures** should be so constructed as to be intelligible without reference to the text. Every table and column should be provided with an explanatory heading. Units of measure must always be clearly indicated.

In the interest of economy and in order to avoid the introduction of errors, tables will be reproduced by photo-offset means directly from the author's typed manuscripts. The guidelines detailed below should be followed:
1. Page size should be 8.5 × 11 in. (or 21 × 30 cm). 2. Large or long tables should be typed on continuing sheets. 3. Table headings should be typed on separate sheets but identifying numbers should be placed on the upper righthand corner of each sheet of tabular material. 4. Original typed tables are required. It will be the author's responsibility to prepare his tables in accordance with this procedure as no facilities exist at the Editorial Office for retyping. The same data should not be published in both tables and figures. The following standard symbols should be used on line drawings since they are easily available to the printers: ○●+×□■△▲◇◆▽▼.

4. **References** are indicated in the text by numbers on the line brackets, and the full reference should be given in a list at the end of the paper in the following form:

1. Barnes R. G., Borsa F. and Peteson D., *J. appl. Phys.* **36,** 940 (1965).
2. Knight W. D., *Solid State Physics* (Edited by F. Seitz and D. Turnbull), Vol. 2, p. 93. Academic Press, New York (1957).

Abbreviations of journal titles should follow those given in *World List of Scientific Periodicals* (1979).

Footnotes, as distinct from literature references, should be indicated by the following symbols—†, ‡, §, ¶, ‖, commencing anew on each page; they should *not* be included in the numbered reference system.

5. Due to the international character of the journal no rigid rules concerning notation and spelling will be observed, but each paper should be consistent within itself as to symbols and units.

The original manuscript and diagrams will be discarded one month after publication unless the Publisher is requested to return the original material to the author.

JOURNAL OF PHYSICS AND CHEMISTRY OF SOLIDS

VOLUME 52 NUMBER 6 1991

CONTENTS

D. P. Bhattacharya and **T. K. Pramanik**	735	Effect of finite energy of deformation-potential acoustic phonons on the temperature of non-equilibrium carriers
C. L. Roy and **Chandan Basu**	745	A relativistic treatment about the existence of band gaps in one-dimensional disordered systems
J. E. Jaffe, Ravindra Pandey and **A. B. Kunz**	755	Correlated Hartree–Fock electronic structure of ZnO and ZnS
Shoichi Nagata, Shuji Ebisu, Tsuyoshi Aochi, Yasuhiro Kinoshita, Susumu Chikazawa and **Kazuhiko Yamaya**	761	Superconductivity in the filamentary conductor $TaSe_3$
V. Rodriguez, M. Couzi and **C. Sourisseau**	769	Valence force fields of the ordered fluoride $CoZrF_6$ in the cubic and rhombohedral phases
J. P. Burger, P. Vajda and **J. N. Daou**	779	Study of structural ordering, Kondo effects and magnetism in CeH_{2+x} with $0 \leqslant x \leqslant 0.65$, through electrical resistivity measurements
H. Raffius, E. Mörsen, B. D. Mosel, W. Müller-Warmuth, T. Hilbich, M. Reehuis, T. Vomhof and **W. Jeitschko**	787	^{57}Fe Mössbauer spectroscopy and some complementary measurements of various ternary iron phosphides
L. Kovács, M. Wöhlecke, A. Jovanović, K. Polgár and **S. Kapphan**	797	Infrared absorption study of the OH vibrational band in $LiNbO_3$ crystals
D. Grientschnig and **W. Sitte**	805	Interpretation of ionic transport properties of some silver chalcogenides
Yanhua Zhou, Andrew J. Campbell and **Dion L. Heinz**	821	Equations of state and optical properties of the high pressure phase of zinc sulfide
Milind Vaidya and **P. H. Umadikar**	827	Magnetic and Mössbauer studies of Sn substituted rare earth iron garnets
	833	Announcement

INDEXED/ABSTRACTED IN *Cam. Sci. Abstr., Chemical Abstracts Service, Current Contents, EIC Intel., Engrg. Ind. Monthly, INSPEC & PASCAL/CNRS Database, SSSA/CISA/ECA/ISMEC*

Published by
PERGAMON PRESS

OXFORD / NEW YORK / FRANKFURT / SEOUL / SYDNEY / TOKYO

ISSN 0022-3697
JPCSAW 52(6) 735–834 (1991)

Printed in Great Britain by BPCC Wheatons Ltd, Exeter

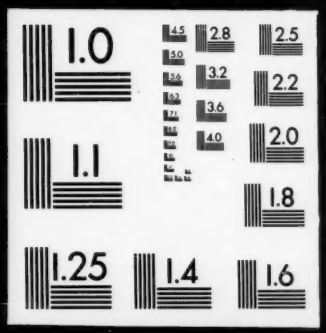
1.0
1.1
1.25
1.4
1.6
1.8
2.0
2.2
2.5
2.8
3.2
3.6
4.0
4.5
5.0
5.6
6.3
7.1
8.0
9.0
10.0
11.2
12.5
14.0
16.0
18.0
20.0
22.4
25.0
28.0
32.0
36.0
40.0
45.0
50.0
56.0
63.0
71.0
80.0
90.0
100.0
112.0
125.0
140.0
160.0
180.0
200.0
224.0
250.0
280.0
320.0
360.0
400.0
450.0
500.0
560.0
630.0
710.0
800.0
900.0
1000.0
1120.0
1250.0
1400.0
1600.0
1800.0
2000.0
2240.0
2500.0
2800.0
3200.0
3600.0
4000.0
4500.0
5000.0
5600.0
6300.0
7100.0
8000.0
9000.0
10000.0
11200.0
12500.0
14000.0
16000.0
18000.0
20000.0
22400.0
25000.0
28000.0
32000.0
36000.0
40000.0
45000.0
50000.0
56000.0
63000.0
71000.0
80000.0
90000.0
100000.0
112000.0
125000.0
140000.0
160000.0
180000.0
200000.0
224000.0
250000.0
280000.0
320000.0
360000.0
400000.0
450000.0
500000.0
560000.0
630000.0
710000.0
800000.0
900000.0
1000000.0
1120000.0
1250000.0
1400000.0
1600000.0
1800000.0
2000000.0
2240000.0
2500000.0
2800000.0
3200000.0
3600000.0
4000000.0
4500000.0
5000000.0
5600000.0
6300000.0
7100000.0
8000000.0
9000000.0
10000000.0
11200000.0
12500000.0
14000000.0
16000000.0
18000000.0
20000000.0
22400000.0
25000000.0
28000000.0
32000000.0
36000000.0
40000000.0
45000000.0
50000000.0
56000000.0
63000000.0
71000000.0
80000000.0
90000000.0
100000000.0
112000000.0
125000000.0
140000000.0
160000000.0
180000000.0
200000000.0
224000000.0
250000000.0
280000000.0
320000000.0
360000000.0
400000000.0
450000000.0
500000000.0
560000000.0
630000000.0
710000000.0
800000000.0
900000000.0
1000000000.0
1120000000.0
1250000000.0
1400000000.0
1600000000.0
1800000000.0
2000000000.0
2240000000.0
2500000000.0
2800000000.0
3200000000.0
3600000000.0
4000000000.0
4500000000.0
5000000000.0
5600000000.0
6300000000.0
7100000000.0
8000000000.0
9000000000.0
10000000000.0
11200000000.0
12500000000.0
14000000000.0
16000000000.0
18000000000.0
20000000000.0
22400000000.0
25000000000.0
28000000000.0
32000000000.0
36000000000.0
40000000000.0
45000000000.0
50000000000.0
56000000000.0
63000000000.0
71000000000.0
80000000000.0
90000000000.0
100000000000.0
112000000000.0
125000000000.0
140000000000.0
160000000000.0
180000000000.0
200000000000.0
224000000000.0
250000000000.0
280000000000.0
320000000000.0
360000000000.0
400000000000.0
450000000000.0
500000000000.0
560000000000.0
630000000000.0
710000000000.0
800000000000.0
900000000000.0
1000000000000.0
1120000000000.0
1250000000000.0
1400000000000.0
1600000000000.0
1800000000000.0
2000000000000.0
2240000000000.0
2500000000000.0
2800000000000.0
3200000000000.0
3600000000000.0
4000000000000.0
4500000000000.0
5000000000000.0
5600000000000.0
6300000000000.0
7100000000000.0
8000000000000.0
9000000000000.0
10000000000000.0
11200000000000.0
12500000000000.0
14000000000000.0
16000000000000.0
18000000000000.0
20000000000000.0
22400000000000.0
25000000000000.0
28000000000000.0
32000000000000.0
36000000000000.0
40000000000000.0
45000000000000.0
50000000000000.0
56000000000000.0
63000000000000.0
71000000000000.0
80000000000000.0
90000000000000.0
100000000000000.0
112000000000000.0
125000000000000.0
140000000000000.0
160000000000000.0
180000000000000.0
200000000000000.0
224000000000000.0
250000000000000.0
280000000000000.0
320000000000000.0
360000000000000.0
400000000000000.0
450000000000000.0
500000000000000.0
560000000000000.0
630000000000000.0
710000000000000.0
800000000000000.0
900000000000000.0
1000000000000000.0
1120000000000000.0
1250000000000000.0
1400000000000000.0
1600000000000000.0
1800000000000000.0
2000000000000000.0
2240000000000000.0
2500000000000000.0
2800000000000000.0
3200000000000000.0
3600000000000000.0
4000000000000000.0
4500000000000000.0
5000000000000000.0
5600000000000000.0
6300000000000000.0
7100000000000000.0
8000000000000000.0
9000000000000000.0
10000000000000000.0
11200000000000000.0
12500000000000000.0
14000000000000000.0
16000000000000000.0
18000000000000000.0
20000000000000000.0
22400000000000000.0
25000000000000000.0
28000000000000000.0
32000000000000000.0
36000000000000000.0
40000000000000000.0
45000000000000000.0
50000000000000000.0
56000000000000000.0
63000000000000000.0
71000000000000000.0
80000000000000000.0
90000000000000000.0
100000000000000000.0
112000000000000000.0
125000000000000000.0
140000000000000000.0
160000000000000000.0
180000000000000000.0
200000000000000000.0
224000000000000000.0
250000000000000000.0
280000000000000000.0
320000000000000000.0
360000000000000000.0
400000000000000000.0
450000000000000000.0
500000000000000000.0
560000000000000000.0
630000000000000000.0
710000000000000000.0
800000000000000000.0
900000000000000000.0
1000000000000000000.0
1120000000000000000.0
1250000000000000000.0
1400000000000000000.0
1600000000000000000.0
1800000000000000000.0
2000000000000000000.0
2240000000000000000.0
2500000000000000000.0
2800000000000000000.0
3200000000000000000.0
3600000000000000000.0
4000000000000000000.0
4500000000000000000.0
5000000000000000000.0
5600000000000000000.0
6300000000000000000.0
7100000000000000000.0
8000000000000000000.0
9000000000000000000.0
10000000000000000000.0
11200000000000000000.0
12500000000000000000.0
14000000000000000000.0
16000000000000000000.0
18000000000000000000.0
20000000000000000000.0
22400000000000000000.0
25000000000000000000.0
28000000000000000000.0
32000000000000000000.0
36000000000000000000.0
40000000000000000000.0
45000000000000000000.0
50000000000000000000.0
56000000000000000000.0
63000000000000000000.0
71000000000000000000.0
80000000000000000000.0
90000000000000000000.0
100000000000000000000.0
112000000000000000000.0
125000000000000000000.0
140000000000000000000.0
160000000000000000000.0
180000000000000000000.0
200000000000000000000.0
224000000000000000000.0
250000000000000000000.0
280000000000000000000.0
320000000000000000000.0
360000000000000000000.0
400000000000000000000.0
450000000000000000000.0
500000000000000000000.0
560000000000000000000.0
630000000000000000000.0
710000000000000000000.0
800000000000000000000.0
900000000000000000000.0
1000000000000000000000.0
1120000000000000000000.0
1250000000000000000000.0
1400000000000000000000.0
1600000000000000000000.0
1800000000000000000000.0
2000000000000000000000.0
2240000000000000000000.0
2500000000000000000000.0
2800000000000000000000.0
3200000000000000000000.0
3600000000000000000000.0
4000000000000000000000.0
4500000000000000000000.0
5000000000000000000000.0
5600000000000000000000.0
6300000000000000000000.0
7100000000000000000000.0
8000000000000000000000.0
9000000000000000000000.0
10000000000000000000000.0
11200000000000000000000.0
12500000000000000000000.0
14000000000000000000000.0
16000000000000000000000.0
18000000000000000000000.0
20000000000000000000000.0
22400000000000000000000.0
25000000000000000000000.0
28000000000000000000000.0
32000000000000000000000.0
36000000000000000000000.0
40000000000000000000000.0
45000000000000000000000.0
50000000000000000000000.0
56000000000000000000000.0
63000000000000000000000.0
71000000000000000000000.0
80000000000000000000000.0
90000000000000000000000.0
100000000000000000000000.0
112000000000000000000000.0
125000000000000000000000.0
140000000000000000000000.0
160000000000000000000000.0
180000000000000000000000.0
200000000000000000000000.0
224000000000000000000000.0
250000000000000000000000.0
280000000000000000000000.0
320000000000000000000000.0
360000000000000000000000.0
400000000000000000000000.0
450000000000000000000000.0
500000000000000000000000.0
560000000000000000000000.0
630000000000000000000000.0
710000000000000000000000.0
800000000000000000000000.0
900000000000000000000000.0
1000000000000000000000000.0
1120000000000000000000000.0
1250000000000000000000000.0
1400000000000000000000000.0
1600000000000000000000000.0
1800000000000000000000000.0
2000000000000000000000000.0
2240000000000000000000000.0
2500000000000000000000000.0
2800000000000000000000000.0
3200000000000000000000000.0
3600000000000000000000000.0
4000000000000000000000000.0
4500000000000000000000000.0
5000000000000000000000000.0
5600000000000000000000000.0
6300000000000000000000000.0
7100000000000000000000000.0
8000000000000000000000000.0
9000000000000000000000000.0
10000000000000000000000000.0
11200000000000000000000000.0
12500000000000000000000000.0
14000000000000000000000000.0
16000000000000000000000000.0
18000000000000000000000000.0
20000000000000000000000000.0
22400000000000000000000000.0
25000000000000000000000000.0
28000000000000000000000000.0
32000000000000000000000000.0
36000000000000000000000000.0
40000000000000000000000000.0
45000000000000000000000000.0
50000000000000000000000000.0
56000000000000000000000000.0
63000000000000000000000000.0
71000000000000000000000000.0
80000000000000000000000000.0
90000000000000000000000000.0
100000000000000000000000000.0
112000000000000000000000000.0
125000000000000000000000000.0
140000000000000000000000000.0
160000000000000000000000000.0
180000000000000000000000000.0
200000000000000000000000000.0
224000000000000000000000000.0
250000000000000000000000000.0
280000000000000000000000000.0
320000000000000000000000000.0
360000000000000000000000000.0
400000000000000000000000000.0
450000000000000000000000000.0
500000000000000000000000000.0
560000000000000000000000000.0
630000000000000000000000000.0
710000000000000000000000000.0
800000000000000000000000000.0
900000000000000000000000000.0
1000000000000000000000000000.0
1120000000000000000000000000.0
1250000000000000000000000000.0
1400000000000000000000000000.0
1600000000000000000000000000.0
1800000000000000000000000000.0
2000000000000000000000000000.0
2240000000000000000000000000.0
2500000000000000000000000000.0
2800000000000000000000000000.0
3200000000000000000000000000.0
3600000000000000000000000000.0
4000000000000000000000000000.0
4500000000000000000000000000.0
5000000000000000000000000000.0
5600000000000000000000000000.0
6300000000000000000000000000.0
7100000000000000000000000000.0
8000000000000000000000000000.0
9000000000000000000000000000.0
10000000000000000000000000000.0
11200000000000000000000000000.0
12500000000000000000000000000.0
14000000000000000000000000000.0
16000000000000000000000000000.0
18000000000000000000000000000.0
20000000000000000000000000000.0
22400000000000000000000000000.0
25000000000000000000000000000.0
28000000000000000000000000000.0
32000000000000000000000000000.0
36000000000000000000000000000.0
40000000000000000000000000000.0
45000000000000000000000000000.0
50000000000000000000000000000.0
56000000000000000000000000000.0
63000000000000000000000000000.0
71000000000000000000000000000.0
80000000000000000000000000000.0
90000000000000000000000000000.0
100000000000000000000000000000.0
112000000000000000000000000000.0
125000000000000000000000000000.0
140000000000000000000000000000.0
160000000000000000000000000000.0
180000000000000000000000000000.0
200000000000000000000000000000.0
224000000000000000000000000000.0
250000000000000000000000000000.0
280000000000000000000000000000.0
320000000000000000000000000000.0
360000000000000000000000000000.0
400000000000000000000000000000.0
450000000000000000000000000000.0
500000000000000000000000000000.0
560000000000000000000000000000.0
630000000000000000000000000000.0
710000000000000000000000000000.0
800000000000000000000000000000.0
900000000000000000000000000000.0
1000000000000000000000000000000.0
1120000000000000000000000000000.0
1250000000000000000000000000000.0
1400000000000000000000000000000.0
1600000000000000000000000000000.0
1800000000000000000000000000000.0
2000000000000000000000000000000.0
2240000000000000000000000000000.0
2500000000000000000000000000000.0
2800000000000000000000000000000.0
3200000000000000000000000000000.0
3600000000000000000000000000000.0
4000000000000000000000000000000.0
4500000000000000000000000000000.0
5000000000000000000000000000000.0
5600000000000000000000000000000.0
6300000000000000000000000000000.0
7100000000000000000000000000000.0
8000000000000000000000000000000.0
9000000000000000000000000000000.0
10000000000000000000000000000000.0
11200000000000000000000000000000.0
12500000000000000000000000000000.0
14000000000000000000000000000000.0
16000000000000000000000000000000.0
18000000000000000000000000000000.0
20000000000000000000000000000000.0
22400000000000000000000000000000.0
25000000000000000000000000000000.0
28000000000000000000000000000000.0
32000000000000000000000000000000.0
36000000000000000000000000000000.0
40000000000000000000000000000000.0
45000000000000000000000000000000.0
50000000000000000000000000000000.0
56000000000000000000000000000000.0
63000000000000000000000000000000.0
71000000000000000000000000000000.0
80000000000000000000000000000000.0
90000000000000000000000000000000.0
100000000000000000000000000000000.0
112000000000000000000000000000000.0
125000000000000000000000000000000.0
140000000000000000000000000000000.0
160000000000000000000000000000000.0
180000000000000000000000000000000.0
200000000000000000000000000000000.0
224000000000000000000000000000000.0
250000000000000000000000000000000.0
280000000000000000000000000000000.0
320000000000000000000000000000000.0
360000000000000000000000000000000.0
400000000000000000000000000000000.0
450000000000000000000000000000000.0
500000000000000000000000000000000.0
560000000000000000000000000000000.0
630000000000000000000000000000000.0
710000000000000000000000000000000.0
800000000000000000000000000000000.0
900000000000000000000000000000000.0
1000000000000000000000000000000000.0
1120000000000000000000000000000000.0
1250000000000000000000000000000000.0
1400000000000000000000000000000000.0
1600000000000000000000000000000000.0
1800000000000000000000000000000000.0
2000000000000000000000000000000000.0
2240000000000000000000000000000000.0
2500000000000000000000000000000000.0
2800000000000000000000000000000000.0
3200000000000000000000000000000000.0
3600000000000000000000000000000000.0
4000000000000000000000000000000000.0
4500000000000000000000000000000000.0
5000000000000000000000000000000000.0
5600000000000000000000000000000000.0
6300000000000000000000000000000000.0
7100000000000000000000000000000000.0
8000000000000000000000000000000000.0
9000000000000000000000000000000000.0
10000000000000000000000000000000000.0
11200000000000000000000000000000000.0
12500000000000000000000000000000000.0
14000000000000000000000000000000000.0
16000000000000000000000000000000000.0
18000000000000000000000000000000000.0
20000000000000000000000000000000000.0
22400000000000000000000000000000000.0
25000000000000000000000000000000000.0
28000000000000000000000000000000000.0
32000000000000000000000000000000000.0
36000000000000000000000000000000000.0
40000000000000000000000000000000000.0
45000000000000000000000000000000000.0
50000000000000000000000000000000000.0
56000000000000000000000000000000000.0
63000000000000000000000000000000000.0
71000000000000000000000000000000000.0
80000000000000000000000000000000000.0
90000000000000000000000000000000000.0
100000000000000000000000000000000000.0
112000000000000000000000000000000000.0
125000000000000000000000000000000000.0
140000000000000000000000000000000000.0
160000000000000000000000000000000000.0
180000000000000000000000000000000000.0
200000000000000000000000000000000000.0
224000000000000000000000000000000000.0
250000000000000000000000000000000000.0
280000000000000000000000000000000000.0
320000000000000000000000000000000000.0
360000000000000000000000000000000000.0
400000000000000000000000000000000000.0
450000000000000000000000000000000000.0
500000000000000000000000000000000000.0
560000000000000000000000000000000000.0
630000000000000000000000000000000000.0
710000000000000000000000000000000000.0
800000000000000000000000000000000000.0
900000000000000000000000000000000000.0
1000000000000000000000000000000000000.0
1120000000000000000000000000000000000.0
1250000000000000000000000000000000000.0
1400000000000000000000000000000000000.0
1600000000000000000000000000000000000.0
1800000000000000000000000000000000000.0
2000000000000000000000000000000000000.0
2240000000000000000000000000000000000.0
2500000000000000000000000000000000000.0
2800000000000000000000000000000000000.0
3200000000000000000000000000000000000.0
3600000000000000000000000000000000000.0
4000000000000000000000000000000000000.0
4500000000000000000000000000000000000.0
5000000000000000000000000000000000000.0
5600000000000000000000000000000000000.0
6300000000000000000000000000000000000.0
7100000000000000000000000000000000000.0
8000000000000000000000000000000000000.0
9000000000000000000000000000000000000.0
10000000000000000000000000000000000000.0
11200000000000000000000000000000000000.0
12500000000000000000000000000000000000.0
14000000000000000000000000000000000000.0
16000000000000000000000000000000000000.0
18000000000000000000000000000000000000.0
20000000000000000000000000000000000000.0
22400000000000000000000000000000000000.0
25000000000000000000000000000000000000.0
28000000000000000000000000000000000000.0
32000000000000000000000000000000000000.0
36000000000000000000000000000000000000.0
40000000000000000000000000000000000000.0
45000000000000000000000000000000000000.0
50000000000000000000000000000000000000.0
56000000000000000000000000000000000000.0
63000000000000000000000000000000000000.0
71000000000000000000000000000000000000.0
80000000000000000000000000000000000000.0
90000000000000000000000000000000000000.0
100000000000000000000000000000000000000.0
112000000000000000000000000000000000000.0
125000000000000000000000000000000000000.0
140000000000000000000000000000000000000.0
160000000000000000000000000000000000000.0
180000000000000000000000000000000000000.0
200000000000000000000000000000000000000.0
224000000000000000000000000000000000000.0
250000000000000000000000000000000000000.0
280000000000000000000000000000000000000.0
320000000000000000000000000000000000000.0
360000000000000000000000000000000000000.0
400000000000000000000000000000000000000.0
450000000000000000000000000000000000000.0
500000000000000000000000000000000000000.0
560000000000000000000000000000000000000.0
630000000000000000000000000000000000000.0
710000000000000000000000000000000000000.0
800000000000000000000000000000000000000.0
900000000000000000000000000000000000000.0
1000000000000000000000000000000000000000.0
1120000000000000000000000000000000000000.0
1250000000000000000000000000000000000000.0
1400000000000000000000000000000000000000.0
1600000000000000000000000000000000000000.0
1800000000000000000000000000000000000000.0
2000000000000000000000000000000000000000.0
2240000000000000000000000000000000000000.0
2500000000000000000000000000000000000000.0
2800000000000000000000000000000000000000.0
3200000000000000000000000000000000000000.0
3600000000000000000000000000000000000000.0
4000000000000000000000000000000000000000.0
4500000000000000000000000000000000000000.0
5000000000000000000000000000000000000000.0
5600000000000000000000000000000000000000.0
6300000000000000000000000000000000000000.0
7100000000000000000000000000000000000000.0
8000000000000000000000000000000000000000.0
9000000000000000000000000000000000000000.0
10000000000000000000000000000000000000000.0
11200000000000000000000000000000000000000.0
12500000000000000000000000000000000000000.0
14000000000000000000000000000000000000000.0
16000000000000000000000000000000000000000.0
18000000000000000000000000000000000000000.0
20000000000000000000000000000000000000000.0
22400000000000000000000000000000000000000.0
25000000000000000000000000000000000000000.0
28000000000000000000000000000000000000000.0
32000000000000000000000000000000000000000.0
36000000000000000000000000000000000000000.0
40000000000000000000000000000000000000000.0
45000000000000000000000000000000000000000.0
50000000000000000000000000000000000000000.0
56000000000000000000000000000000000000000.0
63000000000000000000000000000000000000000.0
71000000000000000000000000000000000000000.0
80000000000000000000000000000000000000000.0
90000000000000000000000000000000000000000.0
100000000000000000000000000000000000000000.0
112000000000000000000000000000000000000000.0
125000000000000000000000000000000000000000.0
140000000000000000000000000000000000000000.0
160000000000000000000000000000000000000000.0
180000000000000000000000000000000000000000.0
200000000000000000000000000000000000000000.0
224000000000000000000000000000000000000000.0
250000000000000000000000000000000000000000.0
280000000000000000000000000000000000000000.0
320000000000000000000000000000000000000000.0
360000000000000000000000000000000000000000.0
400000000000000000000000000000000000000000.0
450000000000000000000000000000000000000000.0
500000000000000000000000000000000000000000.0
560000000000000000000000000000000000000000.0
630000000000000000000000000000000000000000.0
710000000000000000000000000000000000000000.0
800000000000000000000000000000000000000000.0
900000000000000000000000000000000000000000.0
1000000000000000000000000000000000000000000.0
1120000000000000000000000000000000000000000.0
1250000000000000000000000000000000000000000.0
1400000000000000000000000000000000000000000.0
1600000000000000000000000000000000000000000.0
1800000000000000000000000000000000000000000.0
2000000000000000000000000000000000000000000.0
2240000000000000000000000000000000000000000.0
2500000000000000000000000000000000000000000.0
2800000000000000000000000000000000000000000.0
3200000000000000000000000000000000000000000.0
3600000000000000000000000000000000000000000.0
4000000000000000000000000000000000000000000.0
4500000000000000000000000000000000000000000.0
5000000000000000000000000000000000000000000.0
5600000000000000000000000000000000000000000.0
6300000000000000000000000000000000000000000.0
7100000000000000000000000000000000000000000.0
8000000000000000000000000000000000000000000.0
9000000000000000000000000000000000000000000.0
10000000000000000000000000000000000000000000.0
11200000000000000000000000000000000000000000.0
12500000000000000000000000000000000000000000.0
14000000000000000000000000000000000000000000.0
16000000000000000000000000000000000000000000.0
18000000000000000000000000000000000000000000.0
20000000000000000000000000000000000000000000.0
22400000000000000000000000000000000000000000.0
25000000000000000000000000000000000000000000.0
28000000000000000000000000000000000000000000.0
32000000000000000000000000000000000000000000.0
36000000000000000000000000000000000000000000.0
40000000000000000000000000000000000000000000.0
45000000000000000000000000000000000000000000.0
50000000000000000000000000000000000000000000.0
56000000000000000000000000000000000000000000.0
63000000000000000000000000000000000000000000.0
71000000000000000000000000000000000000000000.0
80000000000000000000000000000000000000000000.0
90000000000000000000000000000000000000000000.0
100000000000000000000000000000000000000000000.0
112000000000000000000000000000000000000000000.0
125000000000000000000000000000000000000000000.0
140000000000000000000000000000000000000000000.0
160000000000000000000000000000000000000000000.0
180000000000000000000000000000000000000000000.0
200000000000000000000000000000000000000000000.0
224000000000000000000000000000000000000000000.0
250000000000000000000000000000000000000000000.0
280000000000000000000000000000000000000000000.0
320000000000000000000000000000000000000000000.0
360000000000000000000000000000000000000000000.0
400000000000000000000000000000000000000000000.0
450000000000000000000000000000000000000000000.0
500000000000000000000000000000000000000000000.0
560000000000000000000000000000000000000000000.0
630000000000000000000000000000000000000000000.0
710000000000000000000000000000000000000000000.0
800000000000000000000000000000000000000000000.0
900000000000000000000000000000000000000000000.0
1000000000000000000000000000000000000000000000.0
1120000000000000000000000000000000000000000000.0
1250000000000000000000000000000000000000000000.0
1400000000000000000000000000000000000000000000.0
1600000000000000000000000000000000000000000000.0
1800000000000000000000000000000000000000000000.0
2000000000000000000000000000000000000000000000.0
2240000000000000000000000000000000000000000000.0
2500000000000000000000000000000000000000000000.0
2800000000000000000000000000000000000000000000.0
3200000000000000000000000000000000000000000000.0
3600000000000000000000000000000000000000000000.0
4000000000000000000000000000000000000000000000.0
4500000000000000000000000000000000000000000000.0
5000000000000000000000000000000000000000000000.0
5600000000000000000000000000000000000000000000.0
6300000000000000000000000000000000000000000000.0
7100000000000000000000000000000000000000000000.0
8000000000000000000000000000000000000000000000.0
9000000000000000000000000000000000000000000000.0
10000000000000000000000000000000000000000000000.0
11200000000000000000000000000000000000000000000.0
12500000000000000000000000000000000000000000000.0
14000000000000000000000000000000000000000000000.0
16000000000000000000000000000000000000000000000.0
18000000000000000000000000000000000000000000000.0
20000000000000000000000000000000000000000000000.0
22400000000000000000000000000000000000000000000.0
25000000000000000000000000000000000000000000000.0
28000000000000000000000000000000000000000000000.0
32000000000000000000000000000000000000000000000.0
36000000000000000000000000000000000000000000000.0
40000000000000000000000000000000000000000000000.0
45000000000000000000000000000000000000000000000.0
50000000000000000000000000000000000000000000000.0
56000000000000000000000000000000000000000000000.0
63000000000000000000000000000000000000000000000.0
71000000000000000000000000000000000000000000000.0
80000000000000000000000000000000000000000000000.0
90000000000000000000000000000000000000000000000.0
100000000000000000000000000000000000000000000000.0
112000000000000000000000000000000000000000000000.0
125000000000000000000000000000000000000000000000.0
140000000000000000000000000000000000000000000000.0
160000000000000000000000000000000000000000000000.0
180000000000000000000000000000000000000000000000.0
200000000000000000000000000000000000000000000000.0
224000000000000000000000000000000000000000000000.0
250000000000000000000000000000000000000000000000.0
280000000000000000000000000000000000000000000000.0
320000000000000000000000000000000000000000000000.0
360000000000000000000000000000000000000000000000.0
400000000000000000000000000000000000000000000000.0
450000000000000000000000000000000000000000000000.0
500000000000000000000000000000000000000000000000.0
560000000000000000000000000000000000000000000000.0
630000000000000000000000000000000000000000000000.0
710000000000000000000000000000000000000000000000.0
800000000000000000000000000000000000000000000000.0
900000000000000000000000000000000000000000000000.0
1000000000000000000000000000000000000000000000000.0
1120000000000000000000000000000000000000000000000.0
1250000000000000000000000000000000000000000000000.0
1400000000000000000000000000000000000000000000000.0
1600000000000000000000000000000000000000000000000.0
1800000000000000000000000000000000000000000000000.0
2000000000000000000000000000000000000000000000000.0
2240000000000000000000000000000000000000000000000.0
2500000000000000000000000000000000000000000000000.0
2800000000000000000000000000000000000000000000000.0
3200000000000000000000000000000000000000000000000.0
3600000000000000000000000000000000000000000000000.0
4000000000000000000000000000000000000000000000000.0
4500000000000000000000000000000000000000000000000.0
5000000000000000000000000000000000000000000000000.0
5600000000000000000000000000000000000000000000000.0
6300000000000000000000000000000000000000000000000.0
7100000000000000000000000000000000000000000000000.0
8000000000000000000000000000000000000000000000000.0
9000000000000000000000000000000000000000000000000.0
10000000000000000000000000000000000000000000000000.0
11200000000000000000000000000000000000000000000000.0
12500000000000000000000000000000000000000000000000.0
14000000000000000000000000000000000000000000000000.0
16000000000000000000000000000000000000000000000000.0
18000000000000000000000000000000000000000000000000.0
20000000000000000000000000000000000000000000000000.0
22400000000000000000000000000000000000000000000000.0
25000000000000000000000000000000000000000000000000.0
28000000000000000000000000000000000000000000000000.0
32000000000000000000000000000000000000000000000000.0
36000000000000000000000000000000000000000000000000.0
40000000000000000000000000000000000000000000000000.0
45000000000000000000000000000000000000000000000000.0
50000000000000000000000000000000000000000000000000.0
56000000000000000000000000000000000000000000000000.0
63000000000000000000000000000000000000000000000000.0
71000000000000000000000000000000000000000000000000.0
80000000000000000000000000000000000000000000000000.0
90000000000000000000000000000000000000000000000000.0
100000000000000000000000000000000000000000000000000.0
112000000000000000000000000000000000000000000000000.0
125000000000000000000000000000000000000000000000000.0
140000000000000000000000000000000000000000000000000.0
160000000000000000000000000000000000000000000000000.0
180000000000000000000000000000000000000000000000000.0
200000000000000000000000000000000000000000000000000.0
224000000000000000000000000000000000000000000000000.0
250000000000000000000000000000000000000000000000000.0
280000000000000000000000000000000000000000000000000.0
320000000000000000000000000000000000000000000000000.0
360000000000000000000000000000000000000000000000000.0
400000000000000000000000000000000000000000000000000.0
450000000000000000000000000000000000000000000000000.0
500000000000000000000000000000000000000000000000000.0
560000000000000000000000000000000000000000000000000.0
630000000000000000000000000000000000000000000000000.0
710000000000000000000000000000000000000000000000000.0
800000000000000000000000000000000000000000000000000.0
900000000000000000000000000000000000000000000000000.0
1000000000000000000000000000000000000000000000000000.0
1120000000000000000000000000000000000000000000000000.0
1250000000000000000000000000000000000000000000000000.0
1400000000000000000000000000000000000000000000000000.0
1600000000000000000000000000000000000000000000000000.0
1800000000000000000000000000000000000000000000000000.0
2000000000000000000000000000000000000000000000000000.0
2240000000000000000000000000000000000000000000000000.0
2500000000000000000000000000000000000000000000000000.0
2800000000000000000000000000000000000000000000000000.0
3200000000000000000000000000000000000000000000000000.0
3600000000000000000000000000000000000000000000000000.0
4000000000000000000000000000000000000000000000000000.0
4500000000000000000000000000000000000000000000000000.0
5000000000000000000000000000000000000000000000000000.0
5600000000000000000000000000000000000000000000000000.0
6300000000000000000000000000000000000000000000000000.0
7100000000000000000000000000000000000000000000000000.0
8000000000000000000000000000000000000000000000000000.0
9000000000000000000000000000000000000000000000000000.0
10000000000000000000000000000000000000000000000000000.0
11200000000000000000000000000000000000000000000000000.0
12500000000000000000000000000000000000000000000000000.0
14000000000000000000000000000000000000000000000000000.0
16000000000000000000000000000000000000000000000000000.0
18000000000000000000000000000000000000000000000000000.0
20000000000000000000000000000000000000000000000000000.0
22400000000000000000000000000000000000000000000000000.0
25000000000000000000000000000000000000000000000000000.0
28000000000000000000000000000000000000000000000000000.0
32000000000000000000000000000000000000000000000000000.0
36000000000000000000000000000000000000000000000000000.0
40000000000000000000000000000000000000000000000000000.0
45000000000000000000000000000000000000000000000000000.0
50000000000000000000000000000000000000000000000000000.0
56000000000000000000000000000000000000000000000000000.0
63000000000000000000000000000000000000000000000000000.0
71000000000000000000000000000000000000000000000000000.0
80000000000000000000000000000000000000000000000000000.0
90000000000000000000000000000000000000000000000000000.0
100000000000000000000000000000000000000000000000000000.0
112000000000000000000000000000000000000000000000000000.0
125000000000000000000000000000000000000000000000000000.0
140000000000000000000000000000000000000000000000000000.0
160000000000000000000000000000000000000000000000000000.0
180000000000000000000000000000000000000000000000000000.0
200000000000000000000000000000000000000000000000000000.0
224000000000000000000000000000000000000000000000000000.0
250000000000000000000000000000000000000000000000000000.0
280000000000000000000000000000000000000000000000000000.0
320000000000000000000000000000000000000000000000000000.0
360000000000000000000000000000000000000000000000000000.0
400000000000000000000000000000000000000000000000000000.0
450000000000000000000000000000000000000000000000000000.0
500000000000000000000000000000000000000000000000000000.0
560000000000000000000000000000000000000000000000000000.0
630000000000000000000000000000000000000000000000000000.0
710000000000000000000000000000000000000000000000000000.0
800000000000000000000000000000000000000000000000000000.0
900000000000000000000000000000000000000000000000000000.0
1000000000000000000000000000000000000000000000000000000.0
1120000000000000000000000000000000000000000000000000000.0
1250000000000000000000000000000000000000000000000000000.0
1400000000000000000000000000000000000000000000000000000.0
1600000000000000000000000000000000000000000000000000000.0
1800000000000000000000000000000000000000000000000000000.0
2000000000000000000000000000000000000000000000000000000.0
2240000000000000000000000000000000000000000000000000000.0
2500000000000000000000000000000000000000000000000000000.0
2800000000000000000000000000000000000000000000000000000.0
3200000000000000000000000000000000000000000000000000000.0
3600000000000000000000000000000000000000000000000000000.0
4000000000000000000000000000000000000000000000000000000.0
4500000000000000000000000000000000000000000000000000000.0
5000000000000000000000000000000000000000000000000000000.0
5600000000000000000000000000000000000000000000000000000.0
6300000000000000000000000000000000000000000000000000000.0
7100000000000000000000000000000000000000000000000000000.0
8000000000000000000000000000000000000000000000000000000.0
9000000000000000000000000000000000000000000000000000000.0
10000000000000000000000000000000000000000000000000000000.0
11200000000000000000000000000000000000000000000000000000.0
12500000000000000000000000000000000000000000000000000000.0
14000000000000000000000000000000000000000000000000000000.0
16000000000000000000000000000000000000000000000000000000.0
18000000000000000000000000000000000000000000000000000000.0
20000000000000000000000000000000000000000000000000000000.0
22400000000000000000000000000000000000000000000000000000.0
25000000000000000000000000000000000000000000000000000000.0
28000000000000000000000000000000000000000000000000000000.0
32000000000000000000000000000000000000000000000000000000.0
36000000000000000000000000000000000000000000000000000000.0
40000000000000000000000000000000000000000000000000000000.0
45000000000000000000000000000000000000000000000000000000.0
50000000000000000000000000000000000000000000000000000000.0
56000000000000000000000000000000000000000000000000000000.0
63000000000000000000000000000000000000000000000000000000.0
71000000000000000000000000000000000000000000000000000000.0
80000000000000000000000000000000000000000000000000000000.0
90000000000000000000000000000000000000000000000000000000.0
100000000000000000000000000000000000000000000000000000000.0
112000000000000000000000000000000000000000000000000000000.0
125000000000000000000000000000000000000000000000000000000.0
140000000000000000000000000000000000000000000000000000000.0
160000000000000000000000000000000000000000000000000000000.0
180000000000000000000000000000000000000000000000000000000.0
200000000000000000000000000000000000000000000000000000000.0
224000000000000000000000000000000000000000000000000000000.0
250000000000000000000000000000000000000000000000000000000.0
280000000000000000000000000000000000000000000000000000000.0
320000000000000000000000000000000000000000000000000000000.0
360000000000000000000000000000000000000000000000000000000.0
400000000000000000000000000000000000000000000000000000000.0
450000000000000000000000000000000000000000000000000000000.0
500000000000000000000000000000000000000000000000000000000.0
560000000000000000000000000000000000000000000000000000000.0
630000000000000000000000000000000000000000000000000000000.0
710000000000000000000000000000000000000000000000000000000.0
800000000000000000000000000000000000000000000000000000000.0
900000000000000000000000000000000000000000000000000000000.0
1000000000000000000000000000000000000000000000000000000000.0
1120000000000000000000000000000000000000000000000000000000.0
1250000000000000000000000000000000000000000000000000000000.0
1400000000000000000000000000000000000000000000000000000000.0
1600000000000000000000000000000000000000000000000000000000.0
1800000000000000000000000000000000000000000000000000000000.0
2000000000000000000000000000000000000000000000000000000000.0
2240000000000000000000000000000000000000000000000000000000.0
2500000000000000000000000000000000000000000000000000000000.0
2800000000000000000000000000000000000000000000000000000000.0
3200000000000000000000000000000000000000000000000000000000.0
3600000000000000000000000000000000000000000000000000000000.0
4000000000000000000000000000000000000000000000000000000000.0
4500000000000000000000000000000000000000000000000000000000.0
5000000000000000000000000000000000000000000000000000000000.0
5600000000000000000000000000000000000000000000000000000000.0
6300000000000000000000000000000000000000000000000000000000.0
7100000000000000000000000000000000000000000000000000000000.0
8000000000000000000000000000000000000000000000000000000000.0
9000000000000000000000000000000000000000000000000000000000.0
10000000000000000000000000000000000000000000000000000000000.0
11200000000000000000000000000000000000000000000000000000000.0
12500000000000000000000000000000000000000000000000000000000.0
14000000000000000000000000000000000000000000000000000000000.0
16000000000000000000000000000000000000000000000000000000000.0
18000000000000000000000000000000000000000000000000000000000.0
20000000000000000000000000000000000000000000000000000000000.0
22400000000000000000000000000000000000000000000000000000000.0
25000000000000000000000000000000000000000000000000000000000.0
28000000000000000000000000000000000000000000000000000000000.0
32000000000000000000000000000000000000000000000000000000000.0
36000000000000000000000000000000000000000000000000000000000.0
40000000000000000000000000000000000000000000000000000000000.0
45000000000000000000000000000000000000000000000000000000000.0
50000000000000000000000000000000000000000000000000000000000.0
56000000000000000000000000000000000000000000000000000000000.0
63000000000000000000000000000000000000000000000000000000000.0
71000000000000000000000000000000000000000000000000000000000.0
80000000000000000000000000000000000000000000000000000000000.0
90000000000000000000000000000000000000000000000000000000000.0
100000000000000000000000000000000000000000000000000000000000.0
112000000000000000000000000000000000000000000000000000000000.0
125000000000000000000000000000000000000000000000000000000000.0
140000000000000000000000000000000000000000000000000000000000.0
160000000000000000000000000000000000000000000000000000000000.0
180000000000000000000000000000000000000000000000000000000000.0
200000000000000000000000000000000000000000000000000000000000.0
224000000000000000000000000000000000000000000000000000000000.0
250000000000000000000000000000000000000000000000000000000000.